Journal of Petrology accepted manuscript - 2021-11-25

Identifying crystal accumulation in granitoids through amphibole composition and *in situ* zircon O isotopes in North Qilian Orogen

Shuo Chen[1,2,3*], Yaoling Niu[2,4,5], Xiaohong Wang[1,2,3], Qiqi Xue[1], Wenli Sun[6]

[1] Institute of Oceanology, Chinese Academy of Sciences, Qingdao 266071, China.
[2] Laboratory for Marine Geology, Qingdao National Laboratory for Marine Science and Technology, Qingdao 266061, China
[3] Center for Ocean Mega-Science, Chinese Academy of Sciences, 7 Nanhai Road, Qingdao, 266071, China
[4] Department of Earth Sciences, Durham University, Durham DH1 3LE, UK
[5] China University of Geosciences, Beijing 100083, China
[6] School of Earth and Space Sciences, Peking University, Beijing 100871, China

Corresponding author: Dr. Shuo Chen (shuochen@qdio.ac.cn)

ABSTRACT

Granitoids are the main constituents of the continental crust, and an understanding of their petrogenesis is key to the origin and evolution of continents. Whether crystal fractionation is the dominant way to generate evolved magmas has long been debated, mostly because such processes would produce large volumes of complementary cumulates, which remains elusive. Mafic magmatic enclaves (MMEs) are ubiquitous in granitoids and their presence was initially recognized as cumulates. However, because many MMEs lack obvious evidence of accumulation, such as the classic cumulate textures and modal layering, the cumulate origin of MMEs has been abandoned and the model of magma mixing between mafic and felsic magmas has become popular. In this study, we conduct a combined study of amphibole composition and *in situ* O isotopes in zircons on three suites of orogenic granitoids with MMEs from the North Qilian Orogenic Belt (NQOB). We find that the MMEs and their host granodiorites show overlapping zircon $\delta^{18}O$ values, affirming that they share the same parental magmas. The amphibole compositions indicate that amphiboles from the MMEs are not in equilibrium with a melt whose composition was that of the bulk-rock. These new data, together with the published bulk-rock data, suggest that the MMEs in our study have clear cumulate signatures and are thus of cumulate origin. Our study provide evidence for crystal accumulation in granitoids in the NQOB. This new understanding calls for re-examination on the petrogenesis of some intermediate magmatic rocks (granitoids/andesite) in discussing models of continental crustal growth.

Key words: Mafic magmatic enclaves (MME); Granitoids; Cumulate; Zircon oxygen isotope; Amphibole

INTRODUCTION

The Earth is unique in the solar system in having a buoyant continental crust with an andesitic/dioritic composition (Taylor & McLennan, 1985). Deciphering how

Journal of Petrology accepted manuscript - 2021-11-25

intermediate rocks form is thus a key issue to understand the origin and evolution of continents. It has long been considered that crystal fractionation (coupled with some crustal assimilation) is the dominant mechanism to produce evolved magmas (Deering & Bachmann, 2010). While such process is energetically and mechanically straightforward, it is faced with some problems. Particularly, how to efficiently extract viscous liquids from the crystal mushes and where a complementary reservoir of cumulates exists has remained unclear (Deering & Bachmann, 2010; Gelman *et al.*, 2014; Lee & Morton, 2015). Although cumulate textures in mafic plutons have been documented and widely accepted (Daly, 1933; Irvine, 1982), clear examples of crystal accumulations in intermediate to silicic plutonic rocks have remained elusive, mostly because of ineffective crystal-liquid separation and within-mush crystallization and crystal growth. Thus, it has even been proposed that cumulates are non-existent or rare in silicic batholiths (Glazner *et al.*, 2004; Reubi & Blundy, 2009).

Mafic magmatic enclaves (MMEs) are ubiquitous in granitoids. When studying the Sierra Nevada batholith, the MMEs were initially recognized as "autolith" (Pabst, 1928), which means that they may be "cogenetic" or part of the same system. As implied by "autolith" and on the basis of observations that many MMEs generally show similar mineral assemblages, geochemical trends, ages, and radiogenic isotopes (Sr-Nd-Hf) to their host granitoids, some authors suggested that the MMEs represent the earlier cumulate that was latter disrupted by the incoming magma (e.g., Dodge & Kistler, 1990; Dahlquist, 2002; Niu *et al.*, 2013; Huang *et al.*, 2014; Chen *et al.*, 2015, 2016, 2018; Wang *et al.*, 2016). Opponents of this model, however, cite that the MMEs are generally fine-grained and lack obvious evidence of cumulate texture, such as modal layering, instead suggesting that MMEs are evidence for magma mixing between mafic magmas represented by these MMEs and felsic magmas represented by the host granitoids (see review of Barbarin, 2005). The presence of abundant MMEs bearing plutons has also motivated the hypothesis that magma mixing may be the dominated way to generate andesite (e.g., Eichelberger, 1975). However, whether mixing of mafic magmas with felsic magma is effective enough remains unclear as mafic magmas with higher solidus and liquidus temperatures are likely to solidify after being in contact with felsic melts, which would decrease the efficiency of mixing (eg., Sparks & Marshall, 1986; Caricchi *et al.*, 2012).

Examining whether the MMEs have cumulate signatures is thus critical to understand the mechanism of MME formation, which will also provide new perspectives on the origin of intermediate magmas. Recently, several geochemical models using specific bulk-rock trace element concentrations and ratios has been proposed to identify silicic cumulates, which suggest that many large granitoids are indeed silicic cumulates (Deering & Bachmann, 2010; Gelman *et al.*, 2014; Laurent *et al.*, 2020). Similar conclusion has been made by more recent study by Barnes *et al.* (2019), who used major and trace element compositions of amphiboles to identify silicic cumulates and suggested that bulk-rock compositions of many granitic rocks represent crystal accumulation. These studies imply that bulk-rock and mineral chemistry can provide additional information to facilitate identifying silicic cumulate.

Journal of Petrology accepted manuscript - 2021-11-25

In this study, we report the results of a combined study of amphibole composition and *in situ* O isotopes in zircons on three suites of orogenic granitoids with MMEs from the North Qilian Orogenic Belt (NQOB) (Fig. 1). These new data, together with the recent literature data, indicate that the MMEs in our study are cumulates with clear cumulate signatures in support of the cumulate origin we have been advocating (Niu *et al.*, 2013; Huang *et al.*, 2014; Chen *et al.*, 2015) in general and provide evidence for crystal accumulation in granitoids in the NQOB in particular. This new understanding indicates that some popular views on the petrogenesis of orogenic granitoids in discussing models of continental crustal growth need re-consideration.

GEOLOGICAL BACKGROUND AND SAMPLES

The North Qilian Orogenic Belt (NQOB) is an elongate, NW-SE trending orogenic belt and extends more than 1000 km. It lies between the Alxa Block to the northeast and the Qilian Block to the southwest, (Fig. 1a) and has been suggested as a typical oceanic suture zone comprising Neoproterozoic to Early Paleozoic ophiolite sequences, volcanic and granitic rocks, high pressure (HP) metamorphic rocks, and accretionary complexes (see Song *et al.*, 2013). The southern ophiolite belt (ca. 550-497 Ma) mainly consists of ultramafic cumulate, peridotite and pillow basalts with present-day N-type and E-type mid-ocean ridge basalt (MORB) characteristics (Hou *et al.*, 2006; Song *et al.*, 2019). The northern ophiolite belt (ca. 490-448 Ma) comprises ultramafic rocks, cumulates, MORB, supra-subduction zone (SSZ) basalts, and pelagic-hemipelagic siliceous-argillaceous rocks. While the basaltic rocks in this belt are geochemically similar to present-day N-type MORB, the association with SSZ basalts suggested that they are most likely generated in a back-arc spreading center (Xia *et al.*, 2003; Xia & Song, 2010). The Cambrian-Ordovician arc complex (ca. 516-446 Ma) is located between the two ophiolite belts, which consists of felsic calc-alkaline volcanic rocks, boninitic complexes and granitoid plutons (Xia *et al.*, 2012; Wu *et al.*, 2010; Chen *et al.*, 2014). It has been suggested that the Central Qilian block collided with the Alxa block in the Early Silurian, producing voluminous syn-collisional magmatic rocks of ca. 440 - 420 Ma (Tseng *et al.*, 2009; Song *et al.*, 2013; Yu *et al.*, 2015; Chen *et al.*, 2015, 2016, 2018). The Laohushan (LHS), Qumushan (QMS) and Baojishan (BJS) granitoid plutons (ca. 430 Ma) we studied are located in the eastern segment of the NQOB (Fig. 1b).

A common feature of these syn-collisional granitoids is the ubiquitous MMEs with varying shape and size (a few centimeters to 10's of centimeters in diameter; Fig. 1c-e). Several host-MME sample pairs from the NQOB have been selected for studying *in situ* zircon O isotopes and for studying amphibole composition on representative samples. Petrologically, most MMEs we studied are diorite MMEs (DMME), which generally have a mineral assemblage of amphibole (~30–50 vol%), plagioclase (~40–50 vol%), biotite (~2–20 vol%), quartz (~ 10 vol%), alkali feldspar (<10 vol%) and accessory phases such as zircon, apatite, magnetite, and titanite. These MMEs generally have finer grain-size than their host granodiorites (Fig. 2) (Chen *et al.*, 2015, 2016, 2018). Another type of MMEs are hornblendite MMEs (HMME) in the LHS pluton (Chen *et al.*, 2018), which is dominated by cumulate amphibole with large grain size of

Journal of Petrology accepted manuscript - 2021-11-25

~0.5 to ~6 mm, interstitial plagioclase, clinopyroxene and accessory phases (Fig. 2). These MMEs show neither chilled margins nor textures of crystal resorption or reactive overgrowth. Age dating shows that the MMEs share identical zircon U-Pb ages (~430Ma) to their host granitoids in the three plutons (Fig. 1b).

A TESCAN Integrated Mineral Analyzer (TIMA) system on carbon-coated thin section is used to obtain quantitative mineral modal abundances and distribution maps for the MMEs and their host granodiorites. It can be seen that the MMEs generally have the same mineralogy as their host granodiorites except that they have greater abundances of mafic phases (e.g., amphibole and biotite) (Fig. 3), which confirms our previous estimates (Chen *et al.*, 2015, 2016, 2018). We noted that the clinopyroxene in one LHS HMME (LHS12-06MME) shows higher abundance than previous estimation, however, it is still dominated by amphibole (~64 vol. %; Fig. 3). Another HMME in LHS pluton (LHS12-10MME) shows higher abundance of amphibole (~73% vol.) and less clinopyroxene (~5 vol. %; Fig. 3).

It is important to note that the bulk compositions of the MMEs (i.e., DMMEs and HMMEs) plot in the range of gabbroic diorite, monzogabbro and gabbro in the TAS diagram, which may misguide many to consider the MMEs as representing mantle-derived magmas (Fig. 4). However, the MMEs are not gabbroic rocks, but amphibole-rich diorite or hornblendite. The host granodiorites with MMEs combined, are compositionally calc-alkaline (not shown) and metaluminous to weakly peraluminous (A/CNK = 0.42 to 1.09) (Fig. 4), which is typical of I-type granitoids (Chappell & White, 1992).

METHODS

In situ zircon O isotopes

Zircons of four host-MMEs pairs from three plutons in the NQOB were selected for *in situ* O isotopic analysis. Measurement of oxygen isotopes in zircon was conducted using the Cameca IMS-1280 ion microprobe in the Institute of Geology and Geophysics, Chinese Academy of Sciences. The Cs^+ primary ion beam was accelerated at 10 kV with an intensity of ~ 2-3 nA. The spot size was 10-15 μm. The isotopes ^{16}O and ^{18}O were measured simultaneously using the multi-collection mode on two off-axis Faraday cups, and the mass resolution used was 2500 during the analyses. The instrumental mass fractionation factor (IMF) was corrected using standard zircon Penglai with a $\delta^{18}O$ value of 5.31 ‰ (Li *et al.*, 2009), and measured $^{18}O/^{16}O$ ratios were normalized by using the Vienna Standard Mean Ocean Water composition (VSMOW, $^{18}O/^{16}O$ = 0.0020052). During the analysis, the zircon standard Qinghu was measured as an unknown. Twenty-nine measurements of Qinghu zircon yielded a weighted mean of $\delta^{18}O$ = 5.41 ± 0.67 ‰ (N=29, 2SD; Table S2), which is consistent within error with the reported value of 5.4 ± 0.3 ‰ (2SD) (Li *et al.*, 2009). Detailed analytical techniques and data processing procedures follow Li *et al.* (2009).

Journal of Petrology accepted manuscript - 2021-11-25

Amphibole composition

Amphibole compositions of the MMEs and their host granodiorites of the LHS plutons were analyzed using LA-ICP-MS in the Laboratory of Ocean Lithosphere and Mantle Dynamics at the Institute of Oceanology, Chinese Academy of Sciences. We used a 193 nm ultra-short pulse excimer laser ablation system (Analyte Excite produced by Photon-machines Company) coupled with an Agilent 7900 ICP-MS instrument. Operation conditions of LA-ICP-MS analysis and detailed procedures are given in Xiao *et al.* (2020). Briefly, samples were analyzed using a 40 μm spot size. Fractures and inclusions were carefully avoided. Laser energy density of 3.98 J/cm^2 at a repetition rate of 6 Hz were applied. As amphibole is hydrous, we chose ^{29}Si as the internal standards for data calibration, which were previously analyzed using an electron probe micro-analyzer (EMPA; Chen *et al.*, 2015, 2016, 2018). Every five sample analyses were followed by an analysis of NIST 610 and GSE-1G (NIST 610 was used to correct for the time-dependent drift of sensitivity and mass discrimination). The raw data were processed using ICPMSDataCal 12.0 (Liu *et al.*, 2008). Data quality was assessed by repeated analyses of GSE-1G over the analytical session. The overall precision and accuracy are better than 5% for major elements except for P_2O_5 (14%), and better than 10% for trace elements. The amphibole data for the QMS and BJS plutons were published in Xiao *et al.* (2020) and are compiled in Table S3. Notably, comparison of major element contents obtained using LA-ICP-MS in this study agree well with those previously obtained using EMPA (Chen *et al.*, 2018) (Fig. S1)

Zircon composition

Zircon analysis in thin sections and previous analysis on zircon separates for the QMS, BJS plutons were published in Xiao *et al.* (2020). Previous analysis on zircon separates for LHS pluton were list in Table S4.

Mineral mapping

Mineral/phase maps were obtained on carbon-coated thin sections using a Mira-3 scanning electron microscope equipped with four energy dispersive X-ray spectroscopy (EDS, EDAX Element 30) (TIMA) at Nanjing Hongchuang Geological Exploration Technology Service Co., Ltd. We used an acceleration voltage of 25 kV, probe current of 9 nA. Working distance was set to 15mm. Pixel spacing was set to 3μm and point spacing was set to 9μm. The current and BSE signal intensity were calibrated on a platinum Faraday cup using the automated procedure. EDS performance was checked using manganese standard. The samples were scanned using TIMA liberation analysis module.

RESULTS

Amphibole compositions of the MMEs and their host granodiorites of the LHS plutons are given in Table S2. In the three plutons, the Mg$^{\#}$ values, Al_2O_3 and TiO_2 contents of amphiboles from DMME are similar to those of their host granitoids, except for slightly higher Mg$^{\#}$ values in LHS DMMEs (Fig. 5). In contrast, amphiboles from

Journal of Petrology accepted manuscript - 2021-11-25

the LHS HMME show much higher Al_2O_3 and TiO_2 contents than those of their host granitoids and the DMMEs (Fig. 5). All amphiboles in granodiorites and their MMEs show relatively consistent chondrite-normalized REE patterns that are slightly convex upward, with negative Eu anomalies (Fig. 6).

The *in situ* zircon O isotope data are given in Table 1 and shown in Fig. 7a. Zircons have varying size (50-250 μm) and length/width ratio (~1:1-2:1) with oscillatory zoning in cathodoluminescence (CL) images (Fig. S2), which is consistent with a magmatic origin indicated by Th/U >0.1 (Chen *et al.*, 2015, 2016, 2018). Two host-MME pairs in QMS pluton show identical zircon $\delta^{18}O$ values in the host granodiorites (5.61±0.28‰, n=30, 1σ) and their DMMEs (5.78±0.55‰, n=30, 1σ). Zircons in BJS pluton show similar $\delta^{18}O$ values to QMS pluton in both the host granodiorites (5.93±0.26‰, n=15, 1σ) and their DMME (5.85±0.34‰, n=15, 1σ). Likewise, zircons $\delta^{18}O$ values from LHS host granodiorites (6.74±0.29‰, n=15, 1σ) are also similar to their HMME (7.25±0.53‰, n=12, 1σ) albeit slightly higher than those of BJS and QMS pluton. Notably, while zircon $\delta^{18}O$ values vary slightly for each pluton, zircons from the host granodiorites and their enclosed MMEs of the same pluton generally have indistinguishable $\delta^{18}O$ values (Fig. 7a).

DISCUSSION

Textural constraints on the origin of MMEs.

The 'cumulate' terminology was initially proposed by Wager *et al.* (1960) as a group name for igneous rocks formed by crystal accumulation through settling under gravity, particularly in layered intrusions of basaltic systems. However, it has been later questioned as a number of features in some layered intrusions are not consistent with the concept of crystal settling (e.g., Campbell, 1978). As such, Irvine (1982) re-defined the term 'cumulate' so that crystal settling under gravity is a possible but not essential process in the origin of rocks to which it is applied. Irvine (1982) stated that "*A cumulate is defined as an igneous rock characterized by a cumulus framework of touching mineral crystals or grains that were evidently formed and concentrated primarily through fractional crystallization of their parental magmatic liquids".* While touching crystals with overgrowths and interstitial mineral aggregates are consistent with a cumulate origin, this definition could also apply to granitoids that crystallize without evidence of classic crystal cumulate texture (Vernon & Collins, 2011). Recently, Vernon & Collins (2011) re-defined cumulates as "*igneous rocks that reflect relative concentration of crystals and/or loss of melt and that therefore did not crystallize entirely from a magma of their current whole-rock composition*". They provided some structural criteria to identify whether the current whole-rock composition reflects cumulate processes for granitoids (Vernon & Collins, 2011). Similar definition of cumulate us also given by Barnes *et al.* (2016), who defined cumulate as "*a rock in which the abundance of one or more minerals is in excess of that which would occur during crystallization of a crystal-free parental melt*". In this study, we adopt the definition by Vernon & Collins (2011) to avoid confusion and then use textural and geological evidence to identify cumulate for NQOB MMEs in our

Journal of Petrology accepted manuscript - 2021-11-25

study.

The HMMEs from the LHS pluton have dark color and display typical orthocumulate texture, which is dominated by idiomorphic amphibole with varying grain size (0.5 - 6 mm) and interstitial plagioclase (Fig. 2a, d, Fig. 8j, k, Fig. S3). The host granodiorites from the three plutons are medium grained with lower modal proportion of mafic minerals such as euhedral to subhedral amphibole and biotite (vs, plagioclase) (Fig. 2&8). The typical cumulate texture of HMMEs from the LHS pluton is similar to amphibole-rich enclaves reported in the Gangdese arc (Dong *et al.*, 2020; Zhou *et al.*, 2020), which are interpreted as fragments of igneous cumulates.

While the DMMEs and their host granodiorites from the three plutons lack 'conventional' textural evidence of accumulation, the close association of HMMEs with DMMEs and their host granodiorites both in space and in genesis from the LHS pluton may provide a hint on their origin (see below). Additionally, the DMMEs from the three plutons are fine-grained (0.1 to 2 mm) (Fig. 8), which may imply that they have experienced quench and rapid crystallization (Chen *et al.*, 2016; Rodríguez & Castro, 2017). However, this texture is not incompatible with a cumulate origin because the amphibole, plagioclase and biotite crystals are mostly euhedral to subhedral in the DMMEs on closer inspection (Fig. 8). Laboratory experiments by Rodríguez and Castro (2017) suggested that the cumulates with quenched texture could be formed by fast crystallization and interstitial melt expulsion in a thermal boundary layer with a coupled process of quenching-compaction-accumulation. In fact, the nucleation and growth rates of crystals in magmas is largely determined by the value of effective undercooling ($\Delta T = T_{liquidus} - T_{crystallization}$), which is further controlled by cooling rates (Brandeis & Jaupart, 1987). It has been suggested that cooling rates of 1-10 °C/h could produce non-dendritic, regular crystals of an average size within the range 10-100 μm (Rodríguez & Castro, 2017). In the case of our study, the fine-grain size of DMMEs of ~0.1 to 2 mm implies that the cooling rates of their parental magma is likely not greater than 1 °C/h. As such, it is reasonable to argue that the texture of DMME is not at odd with the abovementioned definition of cumulate. Below, we use compositional evidence to further assess whether the MMEs and their host granodiorites are cognate and whether the MMEs crystallized entirely from a magma parental to their current bulk-rock composition.

In situ zircon O isotopes on the origin of MMEs

Zircon is a ubiquitous accessory mineral in granitoids and is well-understood to be physically and chemically resistant to post-crystallization geological processes, and can thus preserve original geochemical signatures (e.g., Kinny & Maas, 2003). Recent studies suggest that *in situ* zircon U-Pb dating coupled with Hf and/or O isotopes can be a powerful tool to elucidate the nature of magma sources and the role of magma mixing processes in the generation of granitoids if the latter does indeed occur (Kemp *et al.*, 2007; Yang *et al.*, 2007). For example, Yang *et al.* (2007) observed that *in situ* zircon Hf isotopic composition of MMEs [$\varepsilon_{Hf}(t)$ = +4.5 to –6.2] is distinct from the host monzogranite [$\varepsilon_{Hf}(t)$ = –15.1 to –25.4] from the Early Cretaceous Gudaoling batholith (Liaodong Peninsula, NE China), though their zircon U-Pb age was identical. Thus,

Journal of Petrology accepted manuscript - 2021-11-25

they concluded that mixing of mantle-derived mafic magmas with crustal-derived felsic magmas can explain the origin of the MMEs they studied. We should note that this Cretaceous batholith is an intra-plate granitoid of deep continental crustal melting origin that differs from syncollisional granitoids we study here (Niu *et al.*, 2015).

By integrating radiogenic Hf isotope data with stable O isotopes data in zircon, Kemp *et al.* (2007) suggested that the covariant ε_{Hf}-$\delta^{18}O$ zircon arrays represent the progressive interaction between mantle-derived mafic and crustal-derived felsic end-member components during zircon crystallization. In contrast, the MMEs and their host granodiorites in this study show indistinguishable zircon $\delta^{18}O$ values (Fig. 7a), though slightly differs between plutons, implying that they share the same parental magmas. This is consistent with previous inferences based on identical bulk-rock Sr-Nd isotopes between MMEs and their host granodiorites (Fig. 7b, c) (Chen *et al.*, 2015, 2016, 2018). As such, the MMEs in our study argues against the popular model of magma mixing between mantle-derived mafic magmas represented by the MMEs expected to have mantle like $\delta^{18}O$ values (+5.3±0.3 ‰) and crust-derived felsic magmas expected to have elevated $\delta^{18}O$ values (Eiler, 2001; Valley *et al.*, 2005).

Amphibole compositional constraints

It has been suggested that the compositions of amphibole can be used to estimate the crystallization conditions and compositions of its equilibrium melt phase (Ridolfi *et al.*, 2009; Ridolfi & Renzulli, 2011; Putirka, 2016; Zhang *et al.*, 2017; Humphreys *et al.*, 2019). They are also useful for investigating melt differentiation histories and assessing the importance of crystal accumulation and/or melt loss in plutons (Barnes *et al.*, 2019). To test whether equilibrium was achieved between amphiboles and the bulk-rock, we use the following approaches.

First, we performed a test for amphibole-melt Fe-Mg exchange equilibrium, following the approach of Alonso-Perez *et al.* (2009). The Fe-Mg exchange coefficient $K_D(Fe\text{-}Mg)^{Amp\text{-}Melt}$ (hereafter, simply K_D) is defined as:

$$K_D = \frac{X_{FeOt}^{Amp}}{X_{MgO}^{Amp}} / \frac{X_{FeOt}^{Melt}}{X_{MgO}^{Melt}}$$

Where FeOt is total Fe as FeO. As per Alonso-Perez *et al.* (2009), amphibole-melt pairs with $K_D = 0.38 \pm 0.04$ are regarded to be in chemical equilibrium. For comparison, an approach by Putirka (2016) with $K_D = 0.28 \pm 0.11$ is also applied. As shown in Fig. 9, all amphiboles-bulk-rock pairs fall out of Fe-Mg exchange equilibrium field that was calculated by both approaches, suggesting that amphiboles from both the enclaves and their host were not in equilibrium with a melt whose composition was that of the bulk-rock. This implies that neither bulk-rock composition of MMEs nor their host granitoids are representative of melt compositions, but cumulates characterized by amphibole (± biotite) accumulation. In addition, the bulk-rocks of DMMEs from the three plutons display higher $Mg^{\#}$ values than melts in equilibrium with amphiboles, which is similar to those of HMMEs from LHS pluton and amphibole-rich xenoliths from the Gangdanse arc (e.g., Zhou *et al.*, 2020) with a typical cumulate texture. Hence, both

Journal of Petrology accepted manuscript - 2021-11-25

HMME and DMME in this study are accumulations of mainly mafic minerals dominated by amphibole with varying smaller amounts of biotite.

Second, we calculate the rare earth elements (REEs) contents of the melts in equilibrium with amphiboles for each pluton using the amphibole composition (i.e., Ti, Mg, Na, and K contents) and temperature following the model by Shimizu *et al.* (2017), who developed parameterized lattice strain model to calculate REE partition coefficients between amphibole and melt. Briefly, the partition coefficients of REEs between amphibole and melt can be expressed by the following equation based on lattice strain model (Blundy and Wood, 1994):

$$D_i^{Amp-liq} = D_0 \exp\left[-\frac{4\pi EN_A}{RT}\left(\frac{r_0}{2}(r_0-r_i)^2-\frac{1}{3}(r_0-r_i)^3\right)\right] \quad (1)$$

where D_0 and D_i is the strain-free and theoretical amphibole-melt partition coefficient, respectively; r_0 (in angstroms) is the optimum radius of the lattice site; r_i is the ionic radius of the element of interest; E (in GPa) is the effective Young's modulus for the lattice site; N_A is Avogadro's number; R is the universal gas constant (8.3145 J/mol·K); and T is temperature in Kelvin. The lattice strain parameters (D_0, r_0, E) are a function of pressure (P), temperature (T), and composition (X). They were quantified by Shimizu *et al.* (2017) as follows:

$$\ln D_0^{Amp} = -4.21(\pm1.20) + \frac{7.27(\pm0.88)\times10^4}{RT} + 1.52(\pm0.24)X_{Ti}^{Amp} - 0.35(\pm0.06)X_{Mg}^{Amp} - 1.83(\pm0.34)X_{Na}^{Amp} - 2.95(\pm0.34)X_K^{Amp} \quad (2)$$

$$r_0^{Amp} = 1.043(\pm0.004) - 0.039(\pm0.012)X_{Fm}^{Amp-M4} \quad (3)$$

$$E = 337(\pm23) \quad (4)$$

where X_{Ti}^{Amp}, X_{Mg}^{Amp}, X_{Na}^{Amp} and X_K^{Amp} are the number of cations (per 23 oxygen), and X_{Fm}^{Amp-M4} is the total number of cations of Mg, Fe^{2+} and Mn^{2+} in the M4 site, and numbers in parentheses are 2σ uncertainties. Amphibole cation site occupancies and temperature were estimated using the method of Putirka (2016).

As the model we used is independent of melt compositions, it thus would allow estimation of the REE concentration in the melt that is in equilibrium with the amphibole-bearing cumulate, which can provide useful information for understanding the origin of the cumulates. As illustrated in Fig. 6, amphibole from DMME and HMME in each pluton show similar REE patterns to those of their host granodiorites. Hence, the estimated melt in equilibrium with the amphibole from DMME and HMME and their host granodiorites in each pluton show similar REE patterns. Notably, the estimated melt in equilibrium with the amphibole from DMME and HMME display much lower middle-REE (MREE) to heavy-REE (HREE) contents than their bulk-rocks in each pluton, consistent with the inference that both DMME and HMME are amphibole-bearing accumulations with higher MREE to HREE contents.

Journal of Petrology accepted manuscript - 2021-11-25

In sum, the bulk-rock composition of DMME and HMME in this study show much higher $Mg^{\#}$ values and MREE to HREE contents than the melt that in equilibrium with their amphiboles, implying that they are accumulation of mainly mafic minerals dominated by amphibole with varying smaller amount of biotite. This conforms to the definition of cumulate of Vernon & Collins (2011) reasonably well. In contrast, the estimated melt in equilibrium with the amphibole from the host granodiorites in each pluton shows similar REE contents to their bulk-rock composition, which differs from above estimations by amphibole major elements (e.g., $Mg^{\#}$). This discrepancy indicates that the host granodiorites may have experienced melt loss during post-cumulus compaction (see below), which has lower Mg/Fe ratio but similar MREE-HREE contents to the cumulates.

Zircon fractionation record in amphibole composition

It has also been shown that combined analysis of major and trace element of amphibole can be used to determine core-to-rim variation in temperature and melt composition during crystallization (Barnes *et al.*, 2016; Barnes *et al.*, 2019). In our study, we use Ti contents of amphibole as a proxy for decreasing temperature of amphibole crystallization because we observed that Ti in amphibole is closely correlated with temperature (T) (Fig. S4), similar to the observations by Barnes *et al.* (2019). Notably, we use Ti contents as determined by LA-ICP-MS with trace element abundances to reduce systematic bias from different analytical methods (EMPA vs. LA-ICP-MS).

In each pluton, amphiboles from DMMEs and their host granodiorites show similar Zr and Hf concentration ranges, which are linearly correlated with Ti (Fig. 10). In contrast, amphiboles from HMMEs display much higher Ti but lower Zr and Hf contents with limited variation (Fig. 10). More importantly, we find that Zr/Hf ratios of amphiboles from DMMEs and their host granodiorites from the QMS pluton decreases linearly with decreasing Ti, while Zr/Hf ratios of the amphiboles in LHS HMMEs remain almost constant with Ti (Fig. 10). In contrast, Zr/Hf ratios of the amphiboles from BJS DMMEs remain nearly constant at higher Ti but soon decrease with decreasing Ti (Fig. 10). The onset of decreasing Zr/Hf ratios is a strong indicator of zircon fractionation, as zircon is the only common phase capable of causing this decrease (Bea *et al.*, 2006; Barnes *et al.*, 2019). The above observations indicate that zircon is undersaturated during amphibole crystallization to form HMMEs in the LHS pluton, whereas zircon becomes saturated and co-precipitated with amphibole in some DMMEs and their host granodiorites in BJS and QMS pluton.

The above observations are in fact consistent with the trend between bulk-rock Zr and SiO_2 as shown in Fig. 11. It is known that Zr is incompatible in basalt to andesite systems before zircon saturation, but becomes compatible when zircon appears on the liquidus. This change in behavior may provide a potential way to differentiate between liquids and cumulates as previously suggested by Deering & Bachmann (2010). Here three scenarios may account for the three plutons in our study (Fig. 11).

(1) For the LHS pluton, it is assumed that the parent melt is 'M1', which has a basaltic andesite composition as estimated from amphibole composition (Chen

Journal of Petrology accepted manuscript - 2021-11-25

et al., 2018). When amphiboles first crystalized from 'M1', the magma is zircon-undersaturated and Zr is incompatible, thus Zr contents of the residual melt increase until zircon starts to crystallize and a decrease thereafter (Fig. 11a). Accordingly, the earlier cumulates such as LHS HMMEs (and DMMEs) would have lower Zr contents as they are dominated by amphiboles and deficient in zircon.

(2) For the BJS pluton, assuming the parent melt is 'M2' (Fig. 11b), which has a slightly more felsic composition than 'M1'. Zircon is undersaturated but soon reached saturation after crystallization. Thus, the cumulates could also have lower Zr content.

(3) For the QMS pluton, assuming the parent melt is 'M3' (Fig. 11c), which has an andesite to dacite composition as estimated from amphibole composition (Chen *et al.*, 2016). When amphiboles crystalized from melt 'M3', zircon is saturated and Zr is compatible, thus Zr contents in the residual melt decrease. However, as zircon co-precipitated with amphibole in the cumulate assemblages, the cumulate would have higher Zr contents than their parent melt.

It should be noted that although zircon was indeed observed and extracted for dating from HMMEs in previous study (Chen *et al.*, 2018), it might not indicate that zircon can crystallize during earlier HMME formation, because the composition of amphibole and bulk-rock implies that zircon is undersaturated at earlier stage (see above). Furthermore, the zircon composition of the LHS HMME and their host generally show identical REE contents (Fig. 12), indicating that they crystallized from a host magma with similar composition, in contrast to the record by amphibole composition (see above). Thus, we suggest that zircon grains found in LHS HMMEs may be crystallized from later stage, evolved melts and subsequently captured by early formed mafic cumulate piles that are largely plastic before complete solidification. Alternatively, they may be crystallized from evolved interstitial melt that trapped by early formed mafic cumulate piles. While revealing the exact formation mechanism of zircons obtained from mafic igneous rocks is beyond the scope of this study, our above inference appears to be consistent with recent experiments and theoretical calculations, which suggested that basaltic magma is commonly zircon undersaturated and require an anomalously high Zr abundance for the magma to achieve saturation and directly crystallize zircon (Boehnke *et al.*, 2013; Siégel *et al.*, 2018). For instance, quantitative calculations by Siégel *et al.* (2018) suggested that at 900 °C a magma with 45 wt% SiO_2 required >5000 ppm Zr for zircon saturation, and ~700–1800 ppm for 55 wt% SiO_2, which are significantly greater than the typical Zr measured from the bulk-rock (~200-300 ppm). As discussed above, the trends of decreasing ratios of Zr/Hf in amphiboles (Fig. 10) and bulk-rock Zr contents (not shown) in the host granitoids in all the three plutons apparently indicate that zircon is a fractionated phase. Thus, if bulk-rock compositions of the host granitoids can represent the melt composition from which zircon crystallized, the necessary Zr content required to saturate zircon may be calculated at a given temperature. For this calculation, we used two zircon saturation algorithms of Watson and Harrison (1983) and Boehnke *et al.* (2013), following

Journal of Petrology accepted manuscript - 2021-11-25

approaches by Barnes *et al.* (2019). The temperature is estimated at which Zr/Hf decreases in amphibole. As illustrated in Fig. 13, the amount of Zr needed to saturate zircon is much higher than present in the rocks hosting the zircon for both algorithms from Watson & Harrison (1983) and Boehnke et al. (2013). This difference may indicate that Zr-rich melts were lost during accumulation, which further imply that bulk-rock composition of the host granitoids represent crystal-mush, consisting of cumulate phases and trapped melt.

Crystallization models

As a preliminary test for the above crystal accumulation scenario, we used rhyolite-MELTS (Gualda & Ghiorso, 2015) to model crystal-melt equilibria of the LHS host granodiorites and their cumulates following the approach by Lee *et al.* (2015). Calculations were performed for batch crystallization in a closed-system and cooling at constant pressure at 20 °C temperature intervals. A starting composition equivalent to a basaltic andesite was assumed (55.1 wt.% SiO_2, 0.8 wt.% TiO_2, 16.5 wt.% Al_2O_3, 9.1 wt.% $Fe_2O_3^T$, 5.4 wt.% MgO, 6.7 wt.% CaO, 4.2 wt.% Na_2O, 1.6 wt.% K_2O and 0.26 wt.% P_2O_5). Oxygen fugacity was assumed to be buffered at the fayalite-magnetite-quartz buffer. The crystallization conditions of LHS pluton were assumed to be 300 MPa with bulk H_2O of 7 wt.% and 200 MPa with bulk H_2O of 6 wt.%, corresponding to the average Al-in-hornblende pressures for LHS HMME and DMME, respectively (Chen *et al.*, 2018). We compared the modeled geochemical evolution of a crystallizing hydrous basaltic andesite system and the composition of LHS HMME, DMME and their host granodiorites in Fig. 14. We find that the HMMEs and DMMEs with SiO_2 between 45 to 50 wt.% are consistent with being cumulates at model melt fractions of 60-80% (Fig. 14).

In addition, we also plot the experimental results by Moore and Carmichael (1998) in Fig. 14 for comparison. They studied the crystallization products of a basaltic andesite from a Mexican volcanic belt basaltic andesite (55.25 wt. % SiO_2, 0.74 wt. %TiO_2, Al_2O_3, 6.68 wt. % MgO, 5.98 wt. % FeO^t, 7.28 wt. % CaO, 3.97 wt. % Na_2O, 1.18 wt. % K_2O, 0.27 wt. % P_2O_5) at 300 MPa and under hydrous conditions (Moore & Carmichael, 1998). Based on their experimental results, we re-construct the cumulates composition using phase fractions and compositions from minerals and their equilibrium melt by the following equations:

$$C^i_{Bulk\text{-}cum} = X_{liq} \times C^i_{liq} + \sum_{n=1}^{n} X_{Min,n} \times C^i_{Min} \quad (5)$$

$$X_{liq} + \sum_{k=1}^{n} X_{Min,n} = 100\% \quad (6)$$

Where $C^i_{Bulk\text{-}cum}$, C^i_{liq} and C^i_{Min} is the concentration of element *i* in cumulate, interstitial liquid and minerals, respectively; X_{liq} and $X_{Min,n}$ is the phase fraction of interstitial liquid and mineral n, respectively. For simplicity, we assumed that the

Journal of Petrology accepted manuscript - 2021-11-25

composition of interstitial liquid in a cumulate is the same as its equilibrium melt and its fraction is constant (~20 wt.%). As an analogy to HMME, we also construct amphibole-dominated cumulates with 25 wt.% interstitial liquid. It can be seen that there is an overall similarity between the experimental results and LHS MMEs and their host granodiorites, as well as above results of rhyolite-MELTS modeling (Fig. 14). While these similarities are generally in supportive of our preferred model for the cumulate origin of MMEs, we recognize that our MMEs have more modal abundance of amphiboles than those of the rhyolite-MELTS modeling and Moore & Carmichael (1998). This discrepancy may be in part due to inexplicitly of amphibole model in rhyolite-MELTS and/or unmatched starting composition and conditions in the model and the high-pressure experiments (i.e., initial melt composition, pressure, temperature, or water contents) because previous studies have suggested that the stability of amphibole is depending on the H_2O and alkali (Na_2O and K_2O) contents of the bulk composition and pressure (Li *et al.*, 2017). A further well-designed experimental study on these MMEs and their host granodiorites may be of interest for future research.

Formation of the two types of MMEs

Based on the above discussion, we envision the following scenarios for the generation of two types of MMEs and their host granodiorites in this study (Fig.15), which is similar to those suggested by Chen *et al.* (2016) and Rodríguez and Castro (2017). A hydrous magma with basaltic andesite composition intrudes the crust and forms a magma chamber, fractionates amphibole-dominated minerals, which accumulate to the bottom of the magma chamber, as indictaed by blue arrows to form amphibole-riched cumulates similar to LHS HMMEs (Fig. 15). The water-bearing, residual dioritic magmas continues to asend and travels from the shallower magma chamber into the upper crust, during which thermal-mechanical boundary layers are formed at the walls of conduits or new magma chamber leading to differentiation during ascent. Because there is an obvious thermal contrast between the asending magma and the wall rocks, the magma would quench with rapid crystallization. The major liquidus phases of a hydrous dioritic magma would be amphibole, biotite, plagioclase etc. and rapid crystallization will facilitate abundant nucleation without between-nuclei space for rapid growth, thus resulting in the formation of fine-grained cumulates of DMMEs and granodioritic residual magmas (Chen *et al.*, 2015). The granodioritic residual magmas continues to fractionate, generating silicic cumulates similar to the host granidiorite and residual high silica granitic melt, which could evetually form high silica granite or erupt as volcanitc rocks. The earlier crystallized cumulates (HMME and DMME) are later disturbed by subsequent magma replenishment (red arrows), constituting the MMEs in the dominant host granodiorites.

CONCLUDING REMARKS AND IMPLICATIONS

In this study, the texture, amphibole composition, *in situ* zircon O isotopes as well as bulk-rock compositions of the MMEs and their host granodiorites are used to test the hypothesis whether the MMEs in the NQOB are of cumulate origin. New mineral mapping indicates that the texture of DMMEs with fine-grain size from the three

Journal of Petrology accepted manuscript - 2021-11-25

plutons is not incompatible with a cumulate origin as their major constitute crystals are mostly euhedral to subhedral. In each pluton, the overlapping zircon $\delta^{18}O$ values between the MMEs and their host granodiorites suggest that they share the same parental magmas. Taking with published bulk-rock data, we suggest that the MMEs in our study have clear cumulate signatures and cumulate origin. We do not wish to conclude from our studies that MMEs in granitoids are all of cumulate origin worldwide, but we emphasize that MMEs in cyncollisional granitoids are most likely of cumulate origin, which is expected to be further confirmed as already demonstrated by cases such as Pampean Ranges, Sierra Nevada batholith, Gangdese belt and Kunlun Orogen (e.g., Dodge & Kistler, 1990; Dahlquist, 2002; Guan *et al.*, 2012; Huang *et al.*, 2014). All thse share common textural and geochemical characteristics between MMEs and the host granitoids we studied despite their being regarded as evidence for magma mixing with the MMEs representing mantle derived basaltic melts (c.f., Barbarin, 2005). We predict that a comprehensive study through bulk-rock and mineral chemistry will further corroborate the cumulate origin of the MMEs in orogenic granitoids. Importantly, if the abundant MMEs in orogenic granitoids are fully proved not to be evidence of magma mixing (vs. cumulate origin as we understand) as we argue with demonstrations, then it will be important to reconsider the interpretations on the granitoid/andesite petrogenesis, juvenile crust formation and continental crust accretion. In fact, there has been a renewed advocacy in recent studies that crystal accumulation is the dominant process of generating intermediate igneous rocks based on bulk-rock or mineral geochemistry (Deering & Bachmann, 2010; Lee & Morton, 2015; Barnes *et al.*, 2019).

In this context, we should emphasize that it is very likely that MMEs in intraplate granitoids associated with deep crystal anataxis or re-corking may indeed be of magma mixing origin, which needs dedicated investigations.

ACKNOWLEDGMENTS

We thank Prof. Xianhua Li and Qiuli Li for assistance with *in situ* zircon O isotopes. We are grateful to editor Georg Zellmer, Kittrick Rydell Rivera, Mike Dorais, Shuguang Song, Antonio Castro, João Mata and one anonymous reviewer for their constructive comments, which greatly improved the quality of this paper. Financial support for this research was provided by the National Natural Science Foundation (NSFC) grants (41906050, 41630968, 91958215), China Postdoctoral Science Foundation (2019M652496), NSFC-Shandong Joint Fund for Marine Science Research Centers (U1606401), Youth Innovation Promotion Association, Chinese Academy of Sciences (2021206) and 111 project (B18048).

Data Availability Statements

The data underlying this article are available in the article and in its online supplementary material.

Journal of Petrology accepted manuscript - 2021-11-25

REFERENCES

Alonso-Perez, R., Müntener, O. & Ulmer, P. (2009). Igneous garnet and amphibole fractionation in the roots of island arcs: experimental constraints on andesitic liquids. *Contributions to Mineralogy and Petrology* **157**, 541-558.

Barbarin, B. (2005). Mafic magmatic enclaves and mafic rocks associated with some granitoids of the central Sierra Nevada batholith, California: nature, origin, and relations with the hosts. *Lithos* **80**, 155-177.

Barnes, C. G., Coint, N. & Yoshinobu, A. (2016). Crystal accumulation in a tilted arc batholith. *American Mineralogist* **101**, 1719-1734.

Barnes, C. G., Werts, K., Memeti, V. & Ardill, K. (2019). Most granitoid rocks are cumulates: deductions from hornblende compositions and zircon saturation. *Journal of Petrology* **60**, 2227-2240.

Bea, F., Montero, P. & Ortega, M. (2006). A LA–ICP–MS evaluation of Zr reservoirs in common crustal rocks: Implications for Zr and Hf geochemistry, and zircon-forming processes. *The Canadian Mineralogist* **44**, 693-714.

Boehnke, P., Watson, E. B., Trail, D., Harrison, T. M. & Schmitt, A. K. (2013). Zircon saturation re-revisited. *Chemical Geology* **351**, 324-334.

Brandeis, G. & Jaupart, C. (1987). The kinetics of nucleation and crystal growth and scaling laws for magmatic crystallization. *Contributions to Mineralogy to Mineralogy* **96**, 24-34.

Campbell, I. H. (1978). Some problems with the cumulus theory. *Lithos* **11**, 311-323.

Caricchi, L., Annen, C., Rust, A. & Blundy, J. (2012). Insights into the mechanisms and timescales of pluton assembly from deformation patterns of mafic enclaves. *Journal of Geophysical Research: Solid Earth* **117**.

Chappell, B. & White, A. (1992). I-and S-type granites in the Lachlan Fold Belt. *Geological Society of America Special Papers* **272**, 1-26.

Chen, S., Niu, Y., Sun, W., Zhang, Y., Li, J., Guo, P. & Sun, P. (2015). On the origin of mafic magmatic enclaves (MMEs) in syn-collisional granitoids: evidence from the Baojishan pluton in the North Qilian Orogen, China. *Mineralogy and Petrology* **109**, 577-596.

Chen, S., Niu, Y. & Xue, Q. (2018). Syn-collisional felsic magmatism and continental crust growth: A case study from the North Qilian Orogenic Belt at the northern margin of the Tibetan Plateau. *Lithos* **308-309**, 53-64.

Chen, S., Niu, Y. L., Li, J. Y., Sun, W. L., Zhang, Y., Hu, Y. & Shao, F. L. (2016). Syn-collisional adakitic granodiorites formed by fractional crystallization: Insights from their enclosed mafic magmatic enclaves (MMEs) in the Qumushan pluton, North Qilian Orogen at the northern margin of the Tibetan Plateau. *Lithos* **248**, 455-468.

Chen, Y.X., Song, S.G., Niu, Y.L. & Wei, C.J. (2014) Melting of continental crust during subduction initiation: A case study from the Chaidanuo peraluminous granite in the North Qilian suture zone. *Geochimica et Cosmochimica Acta* **132**, 311-336.

Dahlquist, J. (2002). Mafic microgranular enclaves: early segregation from metaluminous magma (Sierra de Chepes), Pampean Ranges, NW Argentina. *Journal of South American Earth Sciences* **15**, 643-655.

Daly, R. A. (1933). Igneous Rocks and the Depths of the Earth.

Deering, C. D. & Bachmann, O. (2010). Trace element indicators of crystal accumulation in silicic igneous rocks. *Earth and Planetary Science Letters* **297**, 324-331.

Journal of Petrology accepted manuscript - 2021-11-25

Dodge, F. & Kistler, R. (1990). Some additional observations on inclusions in the granitic rocks of the Sierra Nevada. *Journal of Geophysical Research: Solid Earth* **95**, 17841-17848.

Dong, X., Niu, Y., Zhang, Z., Tian, Z. & He, Z. (2020). Mesozoic crustal evolution of southern Tibet: Constraints from the early Jurassic igneous rocks in the Central Lhasa terrane. *Lithos* **366-367**.

Eichelberger, J. C. (1975). Origin of andesite and dacite: evidence of mixing at Glass Mountain in California and at other circum-Pacific volcanoes. *Geological Society of America Bulletin* **86**, 1381-1391.

Eiler, J. M. (2001). Oxygen Isotope Variations of Basaltic Lavas and Upper Mantle Rocks. *Reviews in Mineralogy & Geochemistry* **43**, 319-364.

Fu, D., Kusky, T., Wilde, S. A., Polat, A., Huang, B. & Zhou, Z. (2019). Early Paleozoic collision-related magmatism in the eastern North Qilian orogen, northern Tibet: A linkage between accretionary and collisional orogenesis. *Geological Society of America Bulletin* **131**, 1031-1056.

Gelman, S. E., Deering, C. D., Bachmann, O., Huber, C. & Gutiérrez, F. J. (2014). Identifying the crystal graveyards remaining after large silicic eruptions. *Earth and Planetary Science Letters* **403**, 299-306.

Glazner, A. F., Bartley, J. M., Coleman, D. S., Gray, W. & Taylor, R. Z. (2004). Are plutons assembled over millions of years by amalgamation from small magma chambers? *GSA Today* **14**, 4.

Gualda, G. A. R. & Ghiorso, M. S. (2015). MELTS_Excel: AMicrosoft Excel-based MELTS interface for research and teaching of magma properties and evolution. *Geochemistry, Geophysics, Geosystems* **16**, 315-324.

Guan, Q., Zhu, D. C., Zhao, Z. D., Dong, G. C., Zhang, L. L., Li, X. W., Liu, M., Mo, X. X., Liu, Y. S. & Yuan, H. L. (2012). Crustal thickening prior to 38 Ma in southern Tibet: Evidence from lower crust-derived adakitic magmatism in the Gangdese Batholith. *Gondwana Research* **21**, 88-99.

Hou, Q., Chen, Y., Zhao, Z., Zhang, H. & Zhang, B. (2006). Indian Ocean-MORB-type isotopic signature of Yushigou ophiolite in North Qilian Mountains and its implications. *Sci. China. Ser. D Earth Sci.* **49**, 561-572.

Huang, H., Niu, Y., Nowell, G., Zhao, Z., Yu, X., Zhu, D.-C., Mo, X. & Ding, S. (2014). Geochemical constraints on the petrogenesis of granitoids in the East Kunlun Orogenic belt, northern Tibetan Plateau: Implications for continental crust growth through syn-collisional felsic magmatism. *Chemical Geology* **370**, 1-18.

Humphreys, M. C. S., Cooper, G. F., Zhang, J., Loewen, M., Kent, A. J. R., Macpherson, C. G. & Davidson, J. P. (2019). Unravelling the complexity of magma plumbing at Mount St. Helens: a new trace element partitioning scheme for amphibole. *Contributions to Mineralogy and Petrology* **174**.

Irvine, T. (1982). Terminology for layered intrusions. *Journal of Petrology* **23**, 127-162.

Kemp, A., Hawkesworth, C., Foster, G., Paterson, B., Woodhead, J., Hergt, J., Gray, C. & Whitehouse, M. (2007). Magmatic and crustal differentiation history of granitic rocks from Hf-O isotopes in zircon. *Science* **315**, 980-983.

Kinny, P. D. & Maas, R. (2003). Lu–Hf and Sm–Nd isotope systems in zircon. *Reviews in Mineralogy and Geochemistry* **53**, 327-341.

Laurent, O., Björnsen, J., Wotzlaw, J.-F., Bretscher, S., Pimenta Silva, M., Moyen, J.-F., Ulmer, P. & Bachmann, O. (2020). Earth's earliest granitoids are crystal-rich magma reservoirs tapped by silicic eruptions. *Nature Geoscience* **13**, 163-169.

Journal of Petrology accepted manuscript - 2021-11-25

Lee, C.-T. A. & Bachmann, O. (2014). How important is the role of crystal fractionation in making intermediate magmas? Insights from Zr and P systematics. *Earth and Planetary Science Letters* **393**, 266-274.

Lee, C.-T. A. & Morton, D. M. (2015). High silica granites: Terminal porosity and crystal settling in shallow magma chambers. *Earth and Planetary Science Letters* **409**, 23-31.

Lee, C.-T. A., Morton, D. M., Farner, M. J. & Moitra, P. (2015). Field and model constraints on silicic melt segregation by compaction/hindered settling: The role of water and its effect on latent heat release. *American Mineralogist* **100**, 1762-1777.

Li, L., Xiong, X. L. & Liu, X. C. (2017). Nb/Ta Fractionation by Amphibole in Hydrous Basaltic Systems: Implications for Arc Magma Evolution and Continental Crust Formation. *Journal of Petrology*, egw070.

Li, X., Li, W., Wang, X., Li, Q., Liu, Y. & Tang, G. (2009). Role of mantle-derived magma in genesis of early Yanshanian granites in the Nanling Range, South China: in situ zircon Hf-O isotopic constraints. *Science in China Series D: Earth Sciences* **52**, 1262-1278.

Liu, Y., Hu, Z., Gao, S., Gunther, D., Xu, J., Gao, C. & Chen, H. (2008). In situ analysis of major and trace elements of anhydrous minerals by LA-ICP-MS without applying an internal standard. *Chemical Geology* **257**, 34-43.

Moore, G. & Carmichael, I. S. E. (1998). The hydrous phase equilibria (to 3 kbar) of an andesite and basaltic andesite from western Mexico: constraints on water content and conditions of phenocryst growth. *Contributions to Mineralogy and Petrology* **130**, 304-319.

Niu, Y., Liu, Y., Xue, Q., Shao, F., Chen, S., Duan, M., Guo, P., Gong, H., Hu, Y., Hu, Z., Kong, J., Li, J., Liu, J., Sun, P., Sun, W., Ye, L., Xiao, Y. & Zhang, Y. (2015). Exotic origin of the Chinese continental shelf: new insights into the tectonic evolution of the western Pacific and eastern China since the Mesozoic. *Science Bulletin* **60**, 1598-1616.

Niu, Y., Zhao, Z., Zhu, D.-C. & Mo, X. (2013). Continental collision zones are primary sites for net continental crust growth — A testable hypothesis. *Earth-Science Reviews* **127**, 96-110.

Pabst, A. (1928). Observations on inclusions in the granitic rocks of the Sierra Nevada. . *University of California Press* **17**, 325-386.

Putirka, K. (2016). Amphibole thermometers and barometers for igneous systems and some implications for eruption mechanisms of felsic magmas at arc volcanoes. *American Mineralogist* **101**, 841-858.

Reubi, O. & Blundy, J. (2009). A dearth of intermediate melts at subduction zone volcanoes and the petrogenesis of arc andesites. *Nature* **461**, 1269-1273.

Ridolfi, F. & Renzulli, A. (2011). Calcic amphiboles in calc-alkaline and alkaline magmas: thermobarometric and chemometric empirical equations valid up to 1,130°C and 2.2 GPa. *Contributions to Mineralogy and Petrology* **163**, 877-895.

Ridolfi, F., Renzulli, A. & Puerini, M. (2009). Stability and chemical equilibrium of amphibole in calc-alkaline magmas: an overview, new thermobarometric formulations and application to subduction-related volcanoes. *Contributions to Mineralogy and Petrology* **160**, 45-66.

Rodríguez, C. & Castro, A. (2017). Silicic magma differentiation in ascent conduits. Experimental constraints. *Lithos* **272-273**, 261-277.

Shimizu, K., Liang, Y., Sun, C., Jackson, C. R. M. & Saal, A. E. (2017). Parameterized lattice strain models for REE partitioning between amphibole and silicate melt. *American Mineralogist* **102**, 2254-2267.

Journal of Petrology accepted manuscript - 2021-11-25

Siégel, C., Bryan, S. E., Allen, C. M. & Gust, D. A. (2018). Use and abuse of zircon-based thermometers: A critical review and a recommended approach to identify antecrystic zircons. *Earth-Science Reviews* **176**, 87-116.

Song, S., Niu, Y., Su, L. & Xia, X. (2013). Tectonics of the North Qilian orogen, NW China. *Gondwana Research* **23**, 1378-1401.

Song, S.G., Wu, Z.Z., Yang, L.M., Su, L., Xia, X.H., Wang, C., Dong, J.L., Zhou, C.A. & Bi, H.Z. (2019) Ophiolite belts and evolution of the Proto-Tethys Ocean in the Qilian Orogen. *Acta Petrologica Sinica* **35**, 2948-2970. (In Chinese with English abstract)

Sparks, R. & Marshall, L. (1986). Thermal and mechanical constraints on mixing between mafic and silicic magmas. *Journal of Volcanology Geothermal Research* **29**, 99-124.

Taylor, S. R. & McLennan, S. M. (1985). The continental crust: its composition and evolution.

Tseng, C.-Y., Yang, H.-J., Yang, H.-Y., Liu, D., Wu, C., Cheng, C.-K., Chen, C.-H. & Ker, C.-M. (2009). Continuity of the North Qilian and North Qinling orogenic belts, Central Orogenic System of China: Evidence from newly discovered Paleozoic adakitic rocks. *Gondwana Research* **16**, 285-293.

Valley, J. W., Lackey, J. S., Cavosie, A. J., Clechenko, C. C., Spicuzza, M. J., Basei, M. A. S., Bindeman, I. N., Ferreira, V. P., Sial, A. N., King, E. M., Peck, W. H., Sinha, A. K. & Wei, C. S. (2005). 4.4 billion years of crustal maturation: oxygen isotope ratios of magmatic zircon. *Contributions to Mineralogy and Petrology* **150**, 561-580.

Vernon, R. H. & Collins, W. J. (2011). Structural Criteria for Identifying Granitic Cumulates. *The Journal of Geology* **119**, 127-142.

Wager, L., Brown, G. & Wadsworth, W. (1960). Types of igneous cumulates. *Journal of Petrology* **1**, 73-85.

Wang, C., Song, S., Niu, Y., Wei, C. & Su, L. J. J. o. P. (2016). TTG and potassic granitoids in the eastern North China Craton: making Neoarchean upper continental crust during micro-continental collision and post-collisional extension. **57**, 1775-1810.

Watson, E. B. & Harrison, T. M. (1983). Zircon saturation revisited: temperature and composition effects in a variety of crustal magma types. *Earth Planetary Science Letters* **64**, 295-304.

Wu, C.L., Xu, X.Y., Gao, Q.M., Li, X.M., Lei, M., Gao, Y.H., Frost, R.B. & Wooden, J.L., (2010). Early Paleozoic granitoid magmatism and tectonic evolution in North Qilian, NW China. *Acta Petrologica Sinica* **26**, 1027–1044. (In Chinese with English abstract)

Xia, L. Q., Xia, Z. C. & Xu, X. Y. (2003). Magmagenesis in the Ordovician backarc basins of the Northern Oilian Mountains,China. *Geological Society of America Bulletin* **115**, 1510-1522.

Xia, X., Song, S. & Niu, Y. (2012). Tholeiite–Boninite terrane in the North Qilian suture zone: Implications for subduction initiation and back-arc basin development. *Chemical Geology* **328**, 259-277.

Xia, X. H. & Song, S. G. (2010). Forming age and tectono-petrogenises of the Jiugequan ophiolite in the North Qilian Mountain, NW China. *Science Bulletin* **55**, 1899-1907.

Xiao, Y., Chen, S., Niu, Y., Wang, X., Xue, Q., Wang, G., Gao, Y., Gong, H., Kong, J. & Shao, F. (2020). Mineral compositions of syn-collisional granitoids and their implications for the formation of juvenile continental crust and adakitic magmatism. *Journal of Petrology* **61**, egaa038.

Yang, J.-H., Wu, F.-Y., Wilde, S. A., Xie, L.-W., Yang, Y.-H. & Liu, X.-M. (2007). Tracing magma mixing in granite genesis: in situ U–Pb dating and Hf-isotope analysis of zircons. *Contributions to Mineralogy and Petrology* **153**, 177-190.

Journal of Petrology accepted manuscript - 2021-11-25

Yu, S., Zhang, J., Qin, H., Sun, D., Zhao, X., Cong, F. & Li, Y. (2015). Petrogenesis of the early Paleozoic low-Mg and high-Mg adakitic rocks in the North Qilian orogenic belt, NW China: Implications for transition from crustal thickening to extension thinning. *Journal of Asian Earth Sciences* **107**, 122-139.

Zhang, J., Humphreys, M. C. S., Cooper, G. F., Davidson, J. P. & Macpherson, C. G. (2017). Magma mush chemistry at subduction zones, revealed by new melt major element inversion from calcic amphiboles. *American Mineralogist* **102**, 1353-1367.

Zhou, J.-S., Yang, Z.-S., Hou, Z.-Q. & Wang, Q. (2020). Amphibole-rich cumulate xenoliths in the Zhazhalong intrusive suite, Gangdese arc: Implications for the role of amphibole fractionation during magma evolution. *American Mineralogist* **105**, 262-275.

Journal of Petrology accepted manuscript - 2021-11-25

FIGURE CAPTIONS

Fig. 1. (a-b) Simplified geological map of the NQOB showing the main tectonic units and sample locations for this study (after Song *et al.*, 2013; Chen *et al.*, 2018). (c-e) Field photos showing sharp contacts between host rocks and MMEs. Zircon U-Pb ages in b are from the following references: [1] Chen *et al.* (2016); [2] Yu *et al.* (2015); [3] Chen et al., 2015; [4] Chen *et al.* (2018); [5] Fu *et al.* (2019).

Fig. 2. Photomicrographs showing petrographic characteristics of granitoid samples from the LHS (left panels), BJS (middle panels) and QMS pluton (right panels). (a-c) show the contact of MMEs of varying sizes with their host granodiorites. (d-i) show the mineral assemblage of the MMEs (d, g-i) and their granodiorite hosts (e, f). Amp = amphibole; Bt= biotite; Pl = plagioclase; Qz= quartz.

Fig. 3. Mineral abundance (by volumn) of five MME-host pairs from LHS, BJS and QMS pluton by TIMA shows that the MMEs generally have the same mineralogy as their host granodiorites except that they have more abundance of mafic phases (e.g., amphibole and biotite) for each pluton. Mineral abbreviation: Amp = amphibole; Bt= biotite; Pl = plagioclase; Qz= quartz; Chl=chlorite; Cpx=clinopyroxene; Or=orthoclase; Ms=muscovite. Accessory minerals include apatite, titanite, magnetite, pyrite and zircon.

Fig. 4. Classification diagrams of MMEs and their granodiorite hosts from the NQOB. (a) A/NK (molar ratio of Al_2O_3/Na_2O+K_2O) vs. A/CNK (molar ratio of Al_2O_3/Na_2O+K_2O+CaO), and (b) Total alkalis vs. SiO_2. Major elements of the three plutons are from Chen *et al.* (2015, 2016, 2018), which is compiled in Table S1.

Fig. 5. Variation of Al_2O_3 (a) and TiO_2 (b) as a function of $Mg^{\#}$ in amphiboles. Amphibole compostions from MME and the host granodiorites of BJS and QMS pluton are from Xiao *et al.* (2020), which is compiled in Table S3.

Fig. 6. Chondrite-normalized REE patterns for amphiboles from the granodiorite hosts (a, c and e) and their MMEs (b, d, f, and g) from the NQOB. Chondrite REE values are from Sun and McDonough (1989). The solid red line and black lines in each panel represent average compostion of melt in equilibrium with amphiboles, and compostion of bulk-rocks, respectively. The compositions of equilibrium melts are calculated using partition coefficients between amphibole and melt (Shimizu et al., 2017). The red band

Journal of Petrology accepted manuscript - 2021-11-25

represent varing the temperature by ±30° in calculating the compositions of equilibrium melts.

Fig. 7. *In situ* zircon $\delta^{18}O$ (a), bulk-rock $\varepsilon Nd_{(t)}$ (b) and $^{87}Sr/^{86}Sr$ (i) (c) for MMEs and their granodiorite hosts from the NQOB. Bulk-rock $\varepsilon Nd_{(t)}$ (b) and $^{87}Sr/^{86}Sr$ (i) of the three plutons are from Chen *et al.* (2015, 2016, 2018).

Fig. 8. The same region of MMEs imaged by optical microscopy taken under crossed polarized light (XPL), except for LHS HMME in j with taken under plane polarized light (PPL) (left column) and TIMA images, including phase map (middle column) and pie charts of mineral abuandance (by volumn) for the whole thin section of the same MME (right column). The first to third rows are DMME from QMS, BJS and LHS plutons, respectively. The bottem row are LHS HMME.

Fig. 9. Tests for equilibrium between amphibole and melt based on the Fe-Mg exchange coefficient (K_D). K_D values in the range of 0.38± 0.04 (a) (Alonso-Perez *et al.*, 2009) and/or 0.28 ± 0.11 (Putirka 2016) (b) are regarded to be in chemical equilibrium. White squares refer to amphibole-rich cumulate reported in Gangdese arc (Zhou *et al.*, 2020). Other data source are as Fig. 5.

Fig. 10. Variation of Zr, Hf, and Zr/Hf as a function of Ti in amphiboles.

Fig. 11. Plots illustrating predicted concentration of Zr in the melt and complementary cumulates through theoretical liquid lines of descent for LHS pluton (a), BJS pluton (b) and QMS pluton (c). The stars with markers "M1", "M2" and "M3" in different color in each subplot refers to assumed parental magma composition for for LHS pluton (a), BJS pluton (b) and QMS pluton (c), respectively. Bulk-rock Zr vs. SiO_2 are plotted for comparision. See text for details.

Fig. 12. Chondrite-normalized REE patterns of zircons in the host granodiorites and their MMEs. Chondrite REE values are from Sun and McDonough (1989).

Fig. 13. Zr saturation temperatures calculated assuming bulk-rock compositions are equivalent to melt compositions for samples with $2.0 \leqslant M \leqslant 0.9$, using equations from Watson & Harrison (1983) and Boehnke et al. (2013) (enclosed fields).

Fig. 14. (a) Bulk-rock MgO vs SiO_2 for granodiorite hosts and their MMEs from the LHS pluton. Blue and black lines represent isobaric closed system rhyolite-MELTS models (Gualda & Ghiorso, 2015) for the melt (with circle) and cumulate (with square) lines of descent of a parental basaltic andesite composition at 300 MPa with water content of 7 wt% and 300 MPa with water content of 7 wt% , respectively. (b) Bulk-rock MgO of modeled extracted melt and cumulate plotted as a function of residual melt fraction (F%). Color of lines correspond to the same as in a. Arrows indicate direction of cooling and decreasing residual melt fraction. Grey diamonts and black

Journal of Petrology accepted manuscript - 2021-11-25

crosses are compositions of rescructed cumulate and melt from high pressure crystallization experiments of hydrous basaltic andesites (Moore & Carmichael, 1998), respectively. See text for details.

Fig. 15. Cartoon illustrating a possible scenario for MME formation. **a** Hydrous basaltic andesite magma is emplaced and forms a magma chamber, crystallizing amphibole-dominated minerals that sink to the bottom of the magma chamber as indictaed by blue arrows to form amphibole-riched cumulates similar to the LHS HMMEs. **b** Dioritic magmas continues to fractionate amphibole, plagioclase and biotite etc, generating mafic cumulates similar to DMMEs and granodioritic residual magmas. **c** Granodioritic residual magmas continues to fractionate by crystal settling, generating silicic cumulates similar to the host granidiorite and residual high silica granitic melt, which could evetually form high silica granite or erupt as volcanitc rock (d). Earlier crystallized cumulates (HMME and DMME) are later disturbed by subsequent magma replenishment (red arrows), constituting the MMEs in the dominant host granodiorite.

Fig. S1. Comparison of major element contents of amphibole obtained by LA-ICP-MS in this study with those previously obtained by EMPA (Chen *et al.*, 2018).

Fig. S2. Cathodoluminescene (CL) images of zircons from the host granitoids and their MMEs from the NQOB. The red circles indicate the location of O isotope analyses.

Fig. S3. Thin section photos (a) and phase map imaged by TIMA (b) of LHS HMME and its granodiorite showing the HMME is dominated by idiomorphic amphibole with varying grain size and interstitial plagioclase (outlined by white and blue dashed lines). The red line shows the contact of HMME its host granodiorite.

Fig. S4. Variation of Ti as a function of temperature (T °C) in amphiboles. The temperature was calculated from Putirka (2016)

TABLE CAPTIONS

Table 1. Zircon O data for the host granodiorites and their MMEs from NQOB.

Table S1. Summary of bulk-rock compostion for the host granodiorites and their MMEs from NQOB

Table S2. Zircon O data for standard materials during analysis

Table S3. Amphibole compostition for the host granitoids and their MMEs from NQOB.

Table S4. REE concentration of zircon separates for the host granodiorites and their MMEs from NQOB

Figure 1

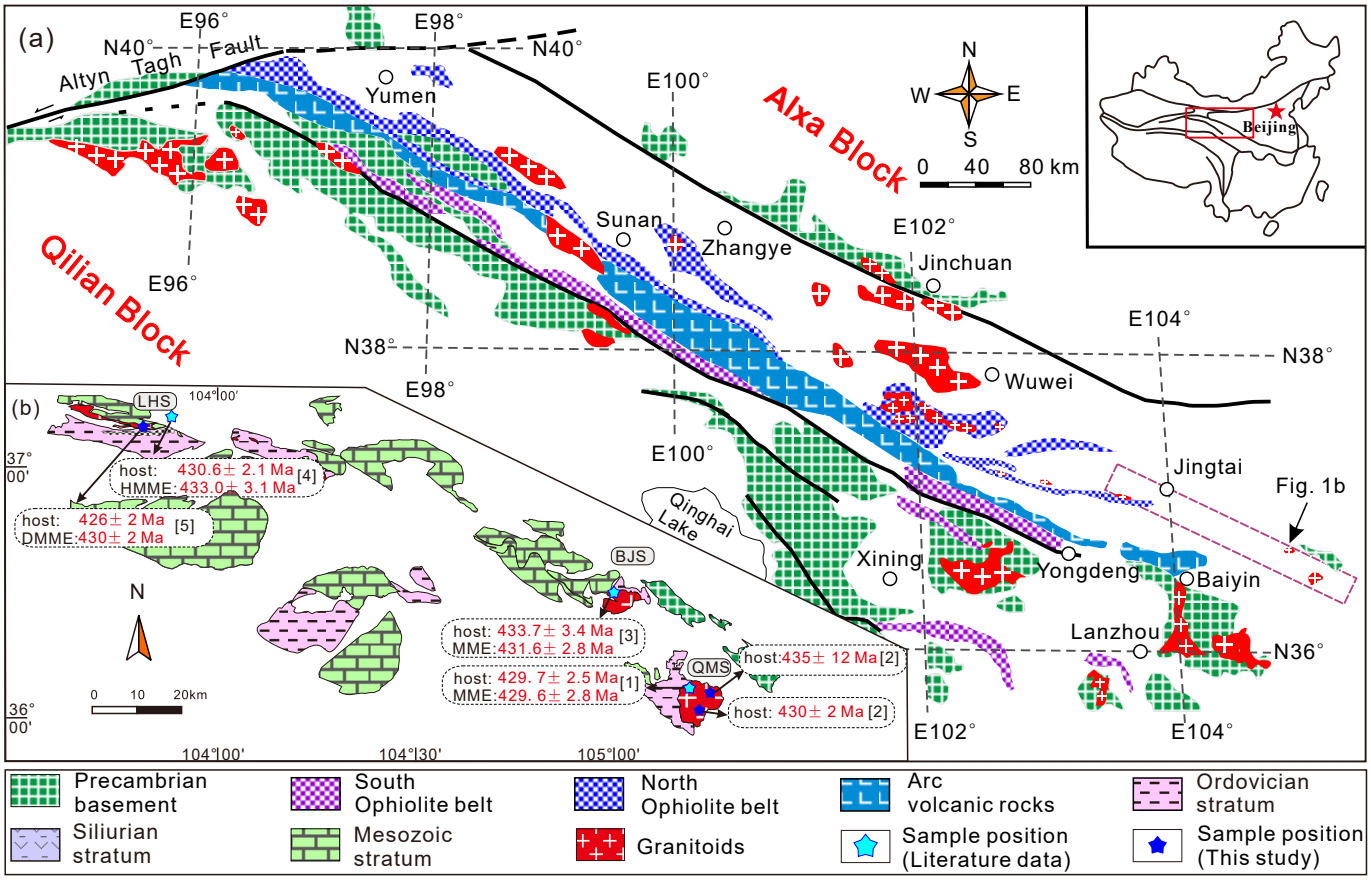

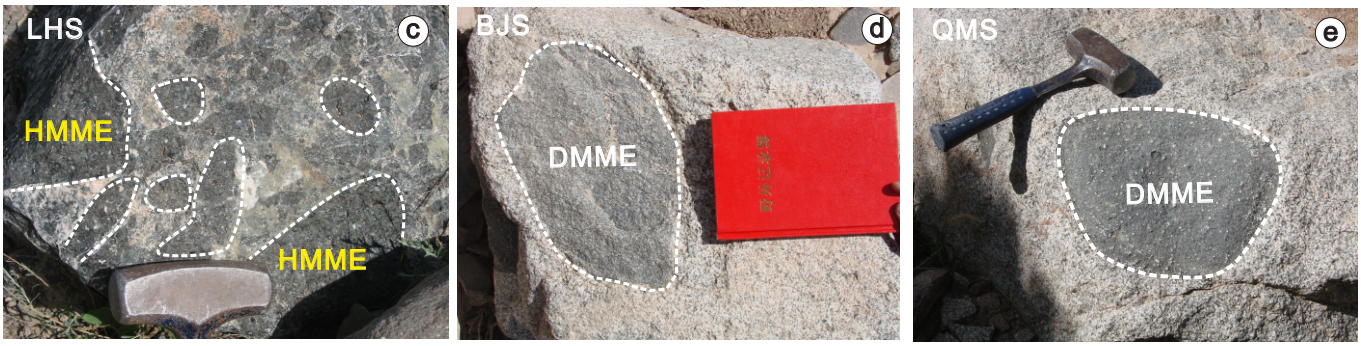

Journal of Petrology accepted manuscript - 2021-11-25

Figure 2

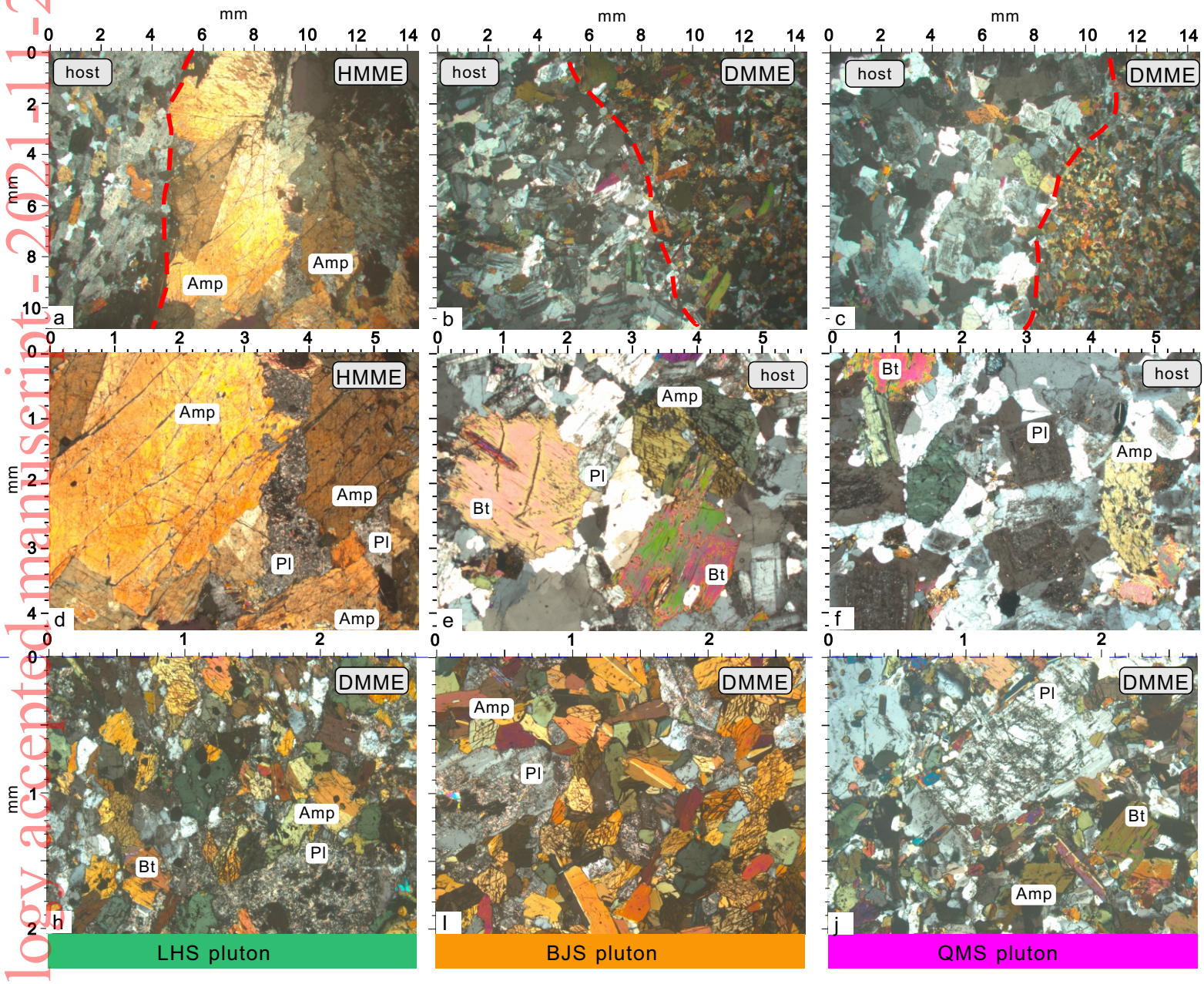

Journal of Petrology accepted manuscript - 2021-11-25

Figure 3

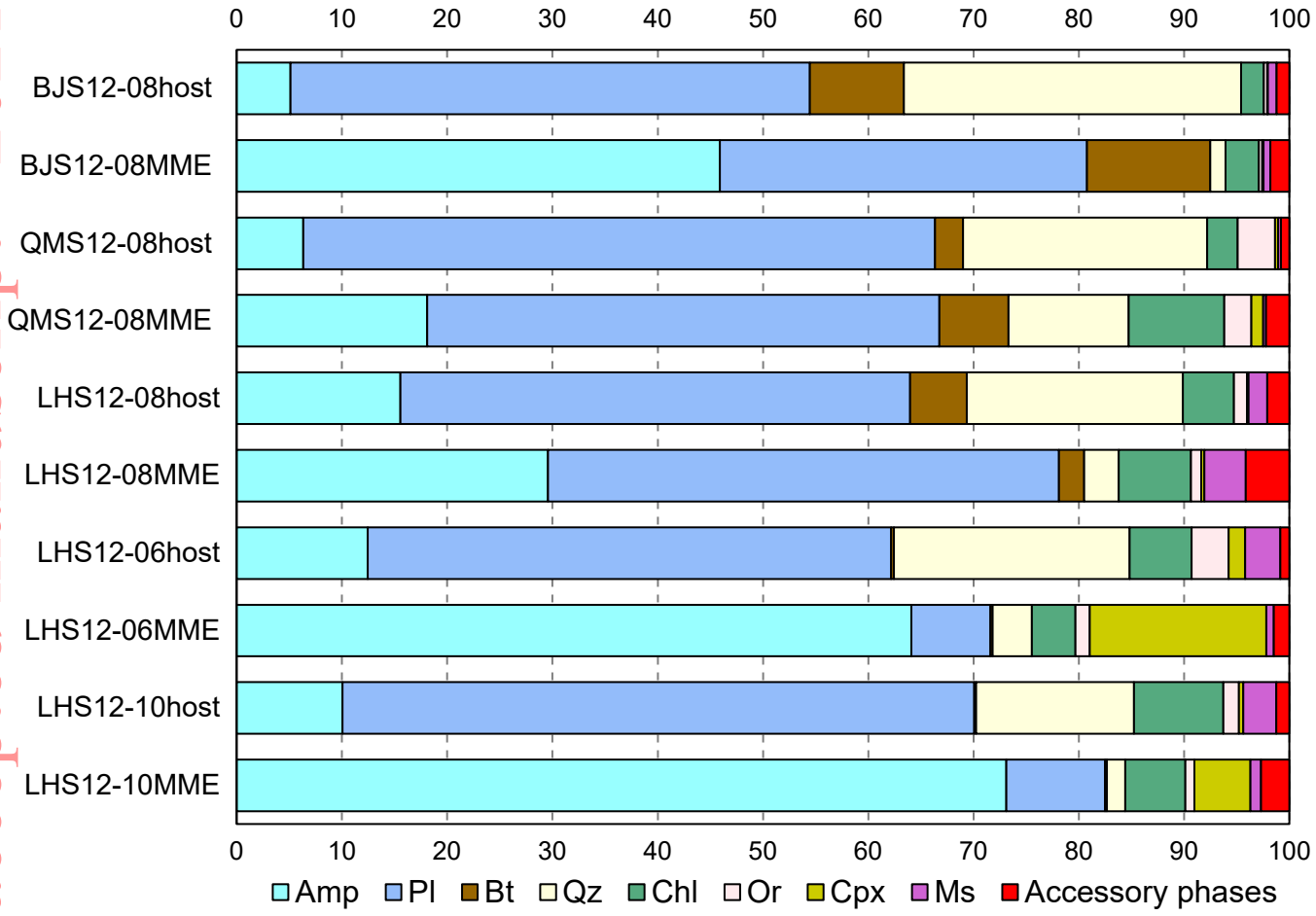

Journal of Petrology accepted manuscript - 2021-11-25

Figure 4

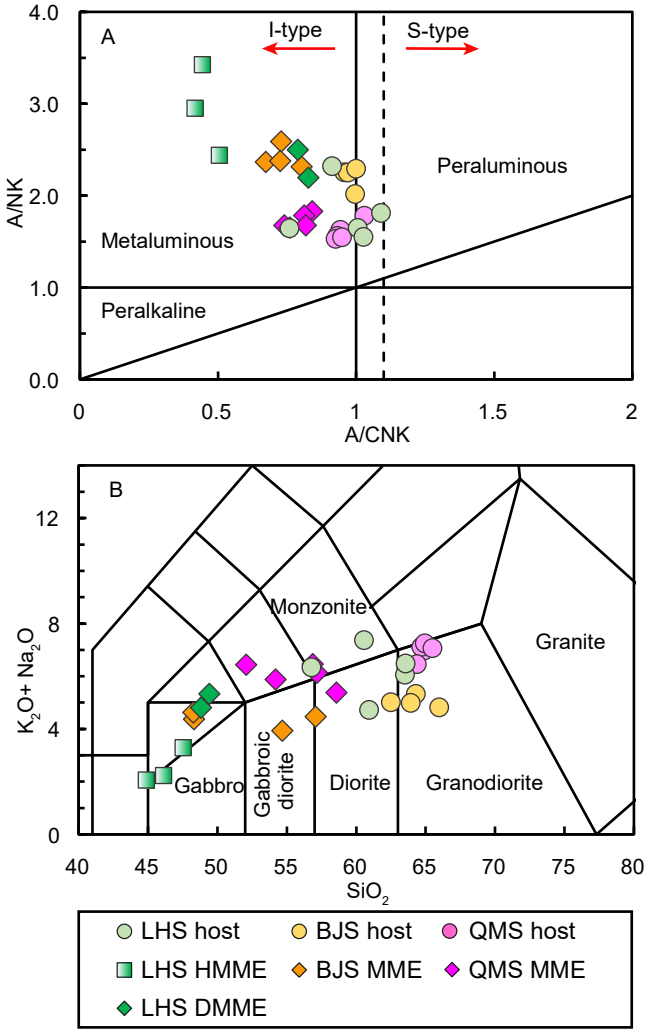

Journal of Petrology accepted manuscript - 2021-11-25

Figure 5

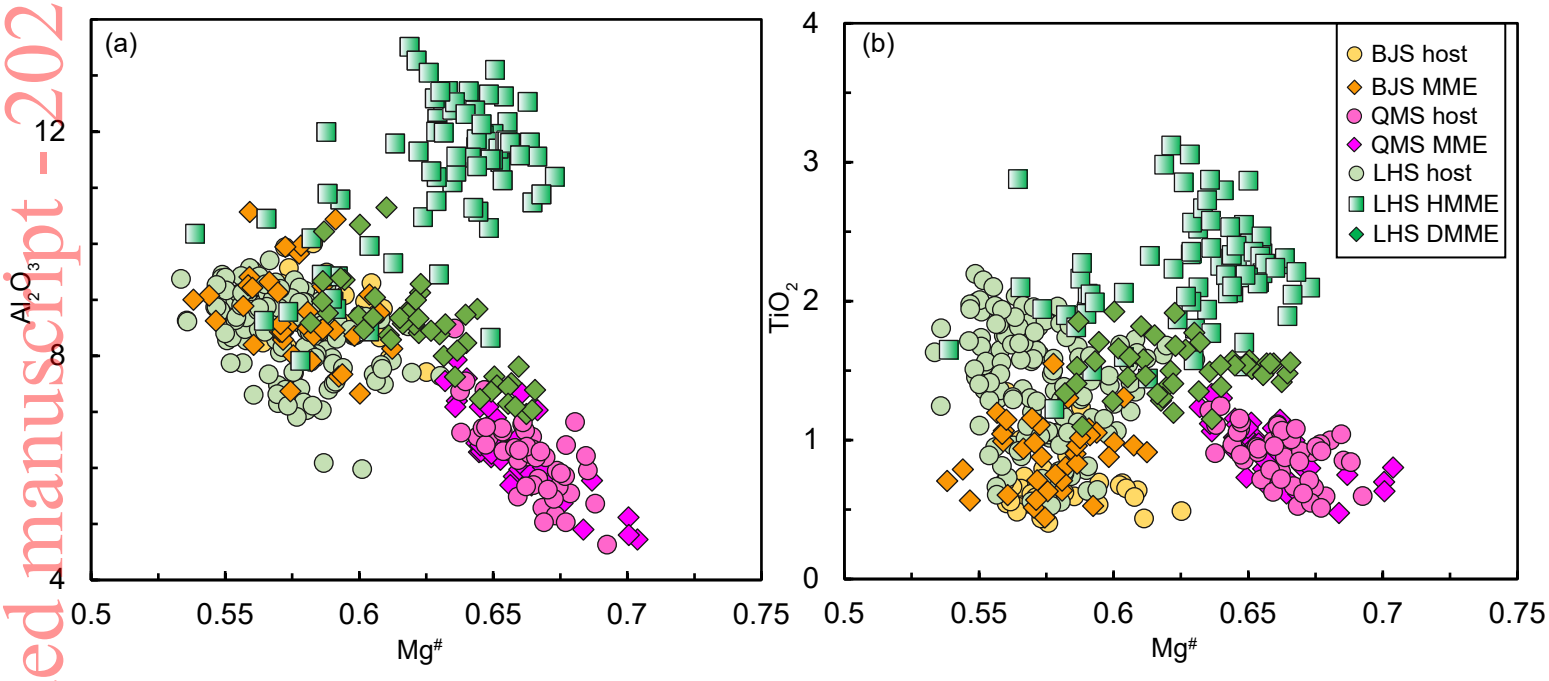

Journal of Petrology accepted manuscript - 2021-11-25

Figure 6

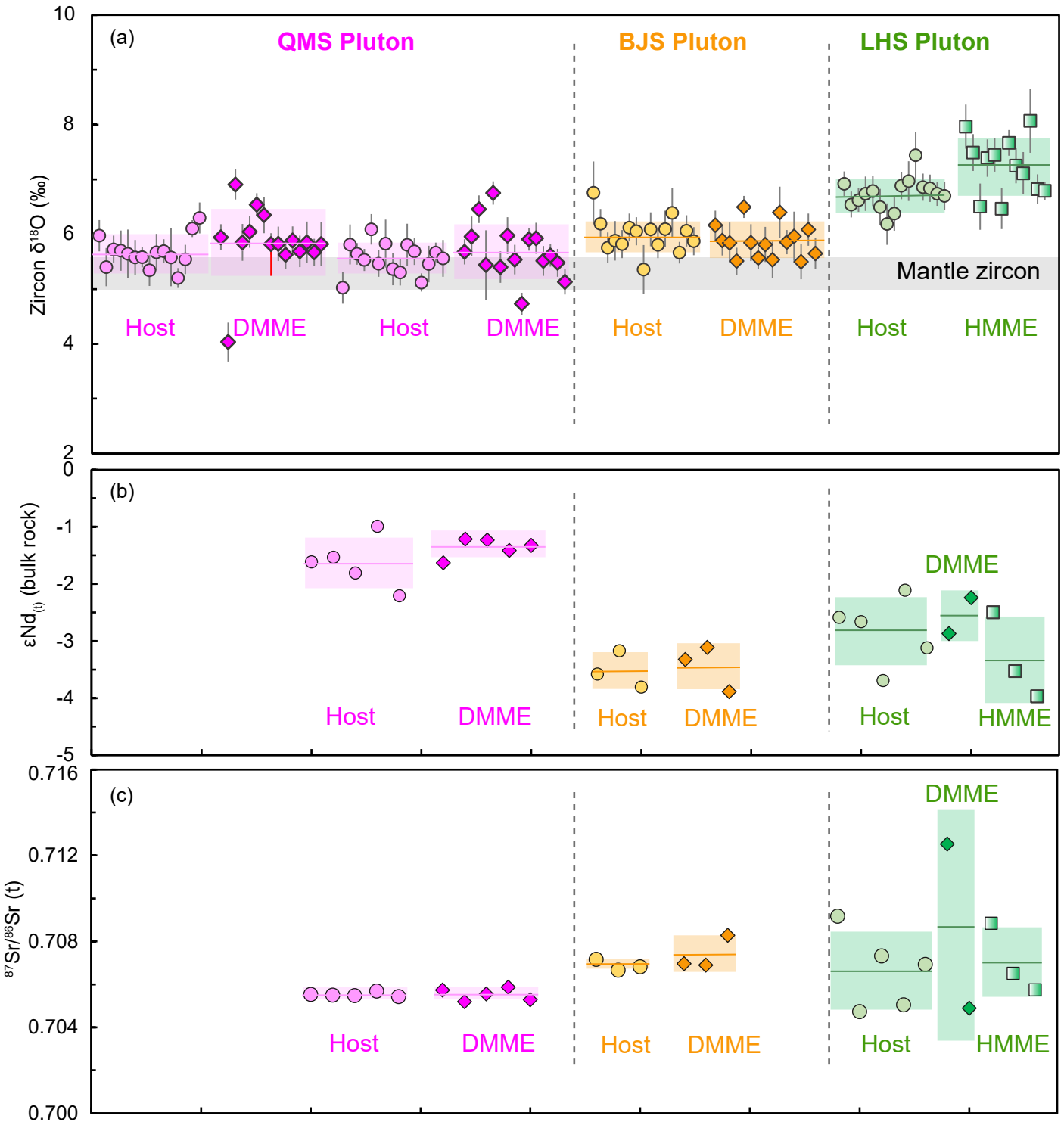

Journal of Petrology accepted manuscript - 2021-11-25

Figure 7

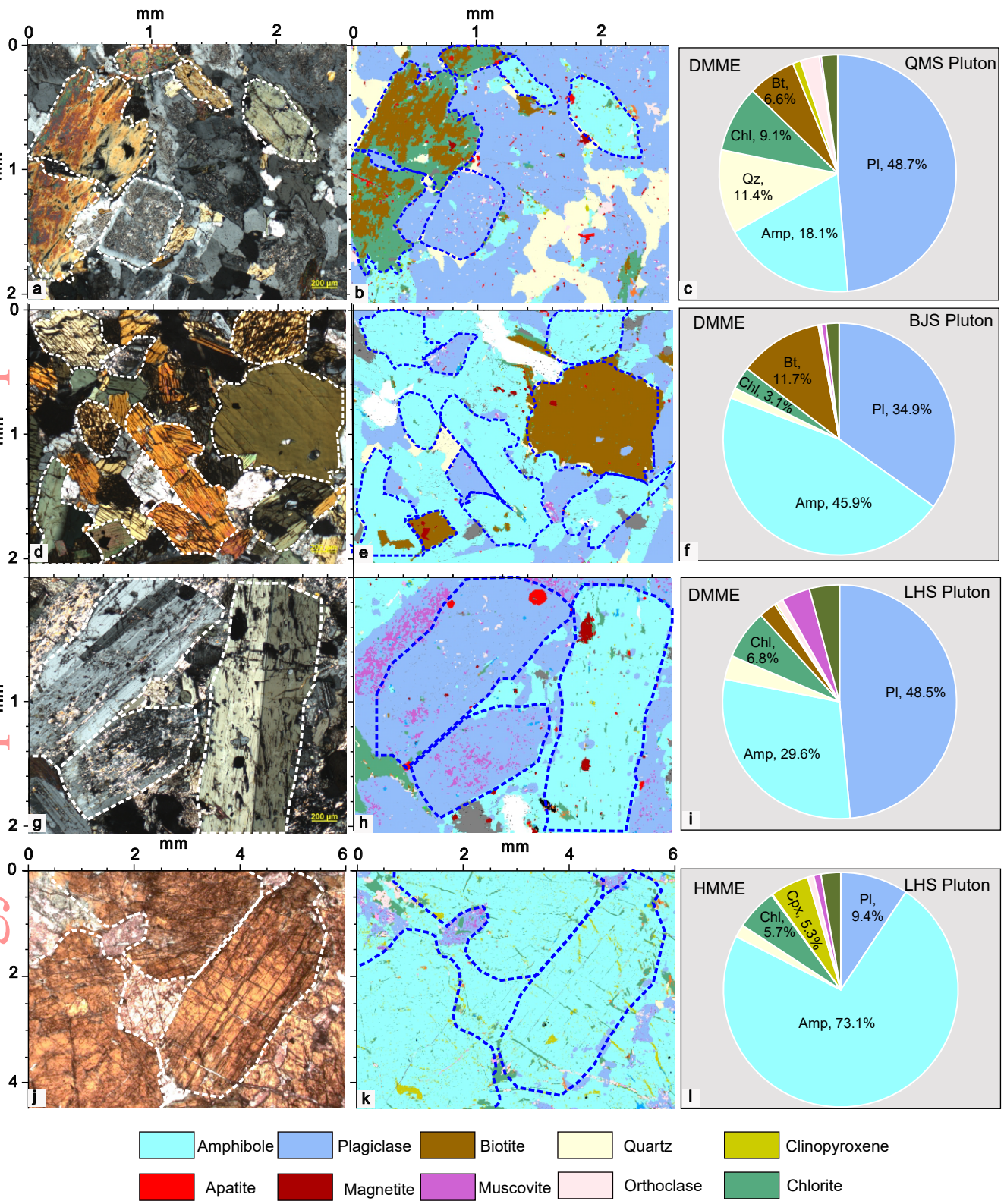

Journal of Petrology accepted manuscript - 2021-11-25

Figure 8

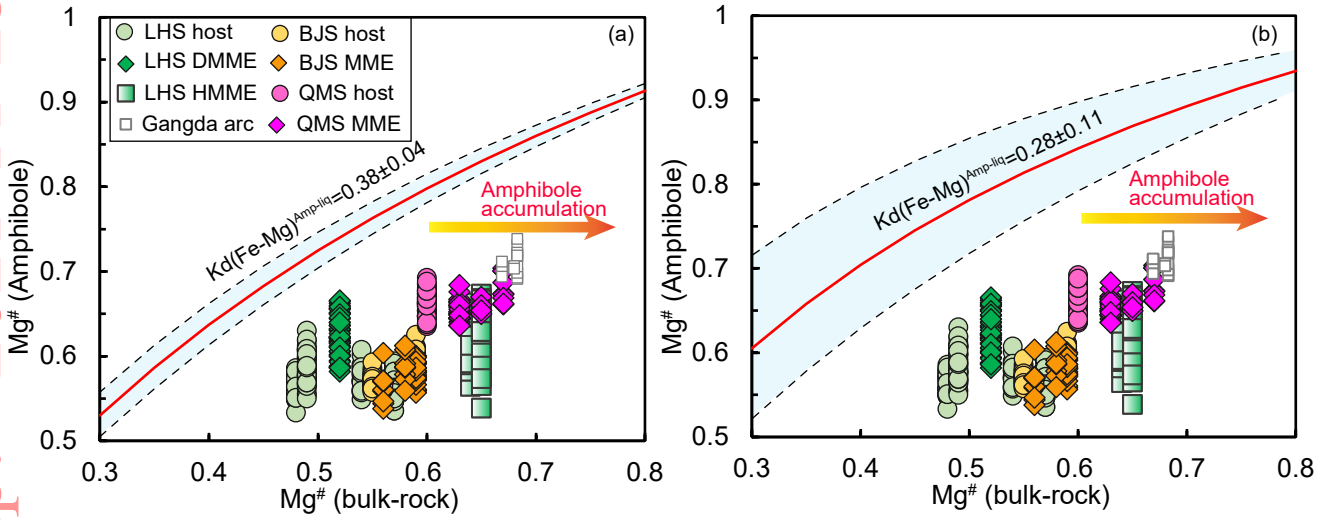

Journal of Petrology accepted manuscript - 2021-11-25

Figure 9

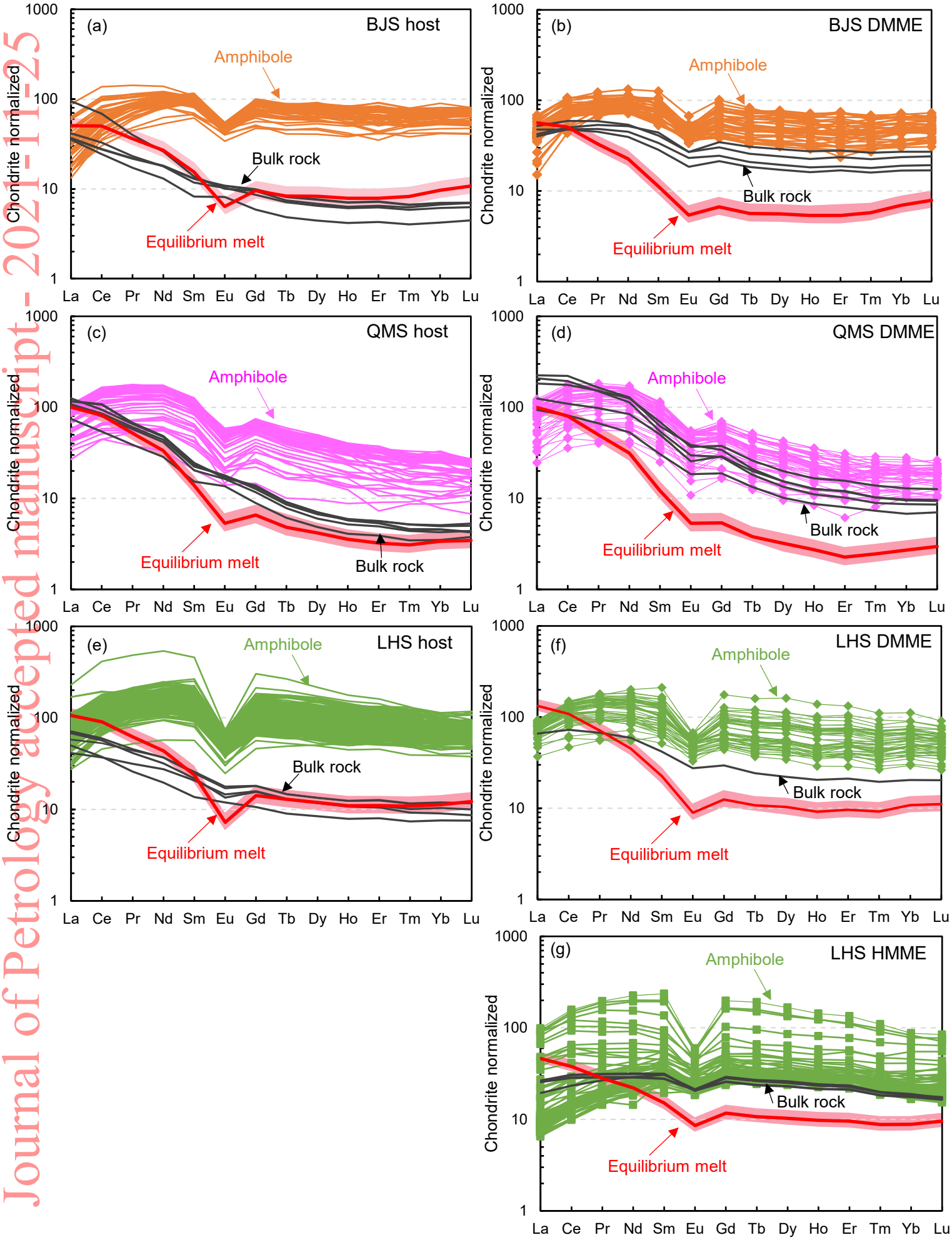

Journal of Petrology accepted manuscript - 2021-11-25

Figure 10

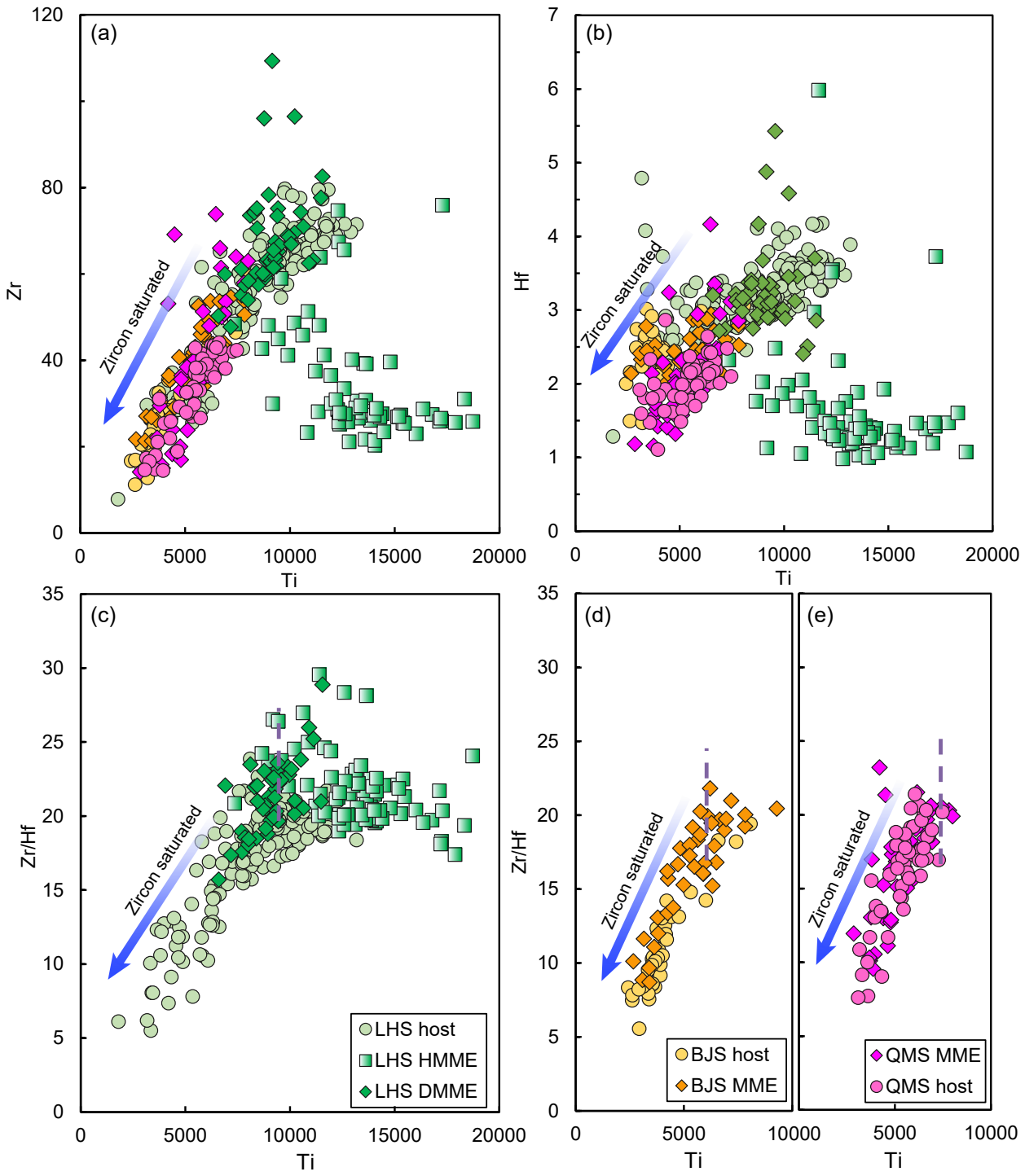

Journal of Petrology accepted manuscript - 2021-11-25

Figure 11

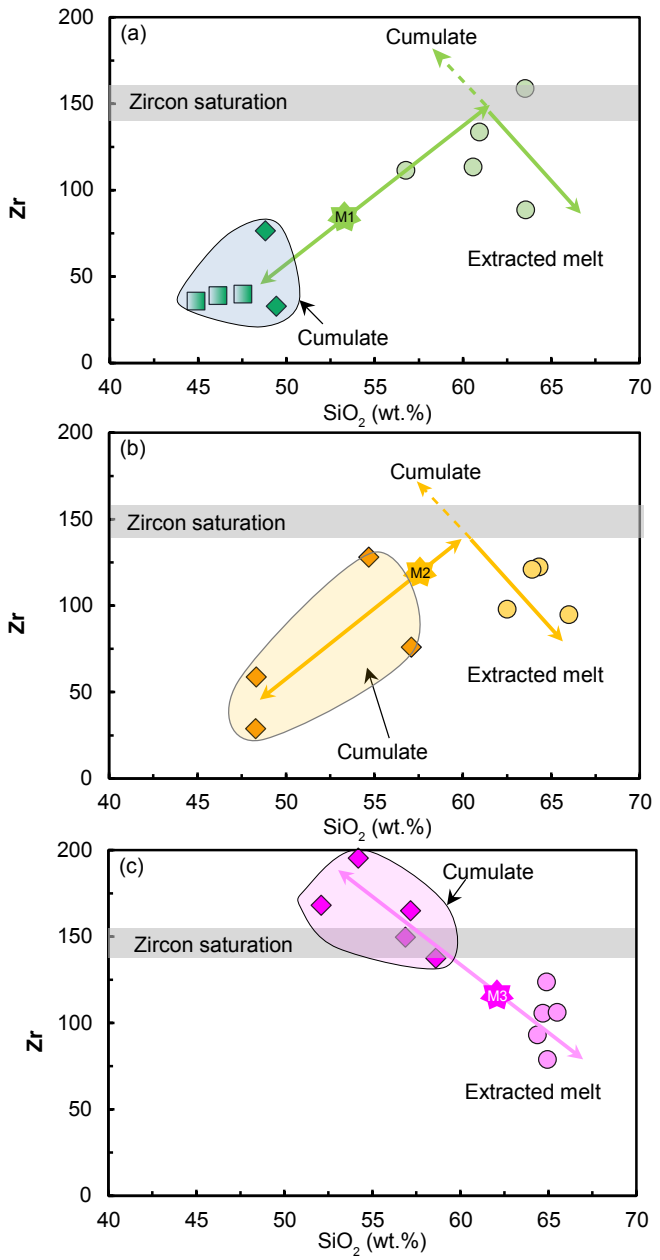

Journal of Petrology accepted manuscript - 2021-11-25

Figure 12

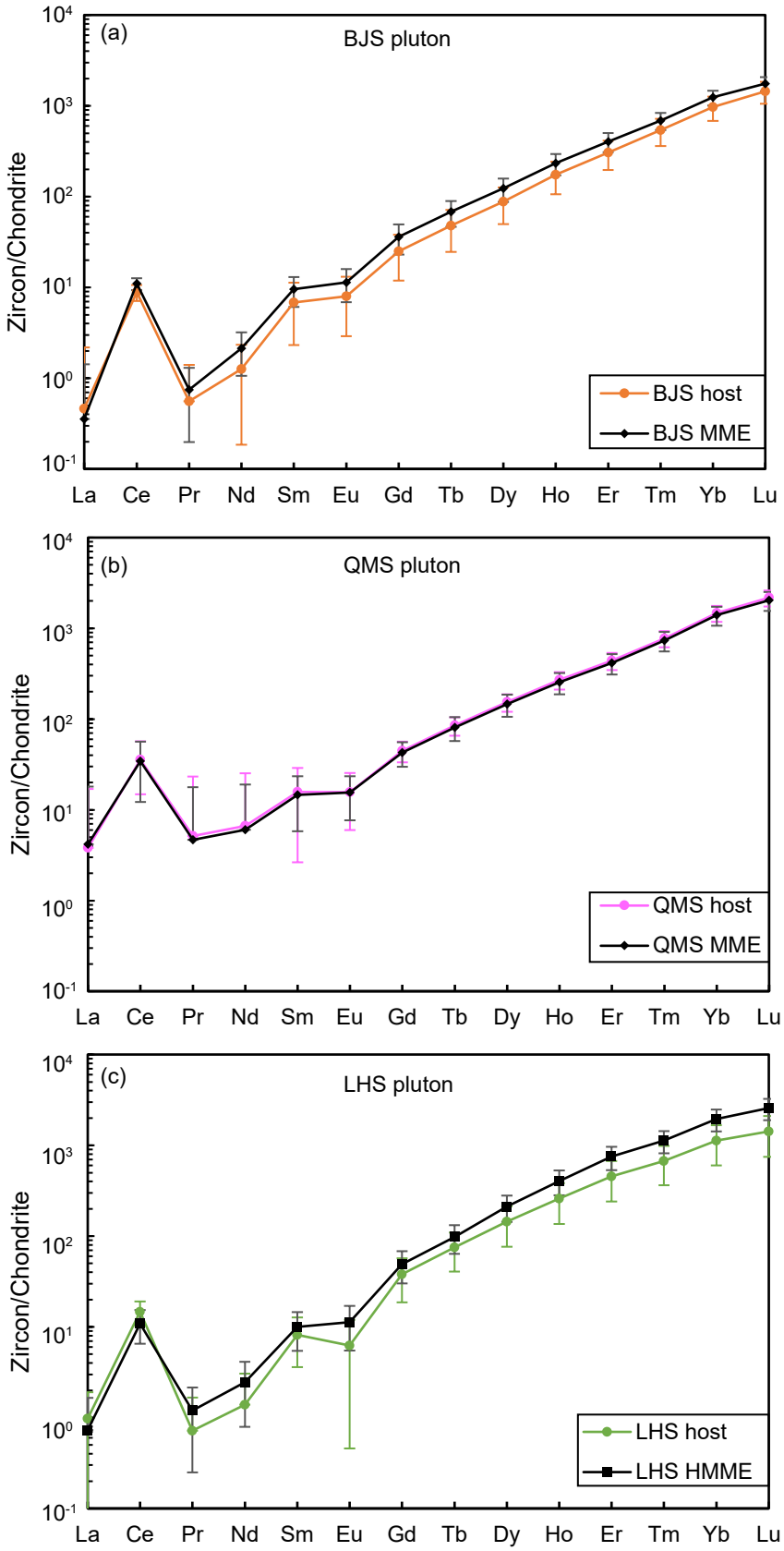

Journal of Petrology accepted manuscript - 2021-11-25

Journal of Petrology accepted manuscript - 2021-11-25

Figure 13

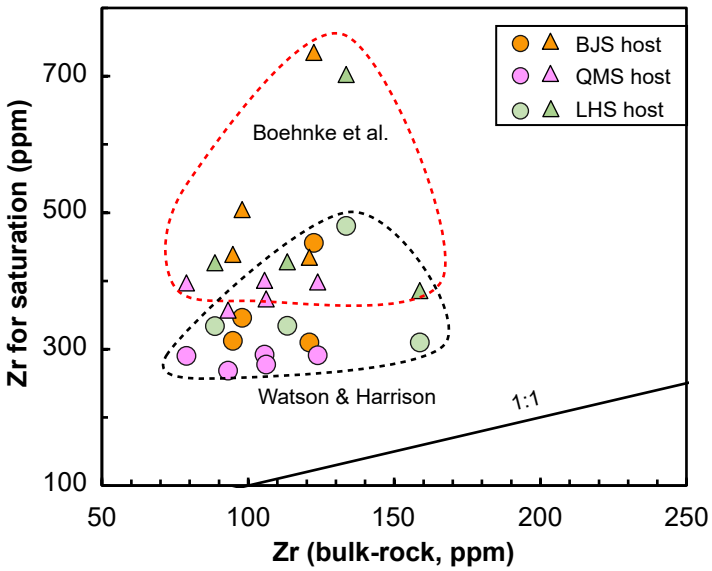

Figure 14

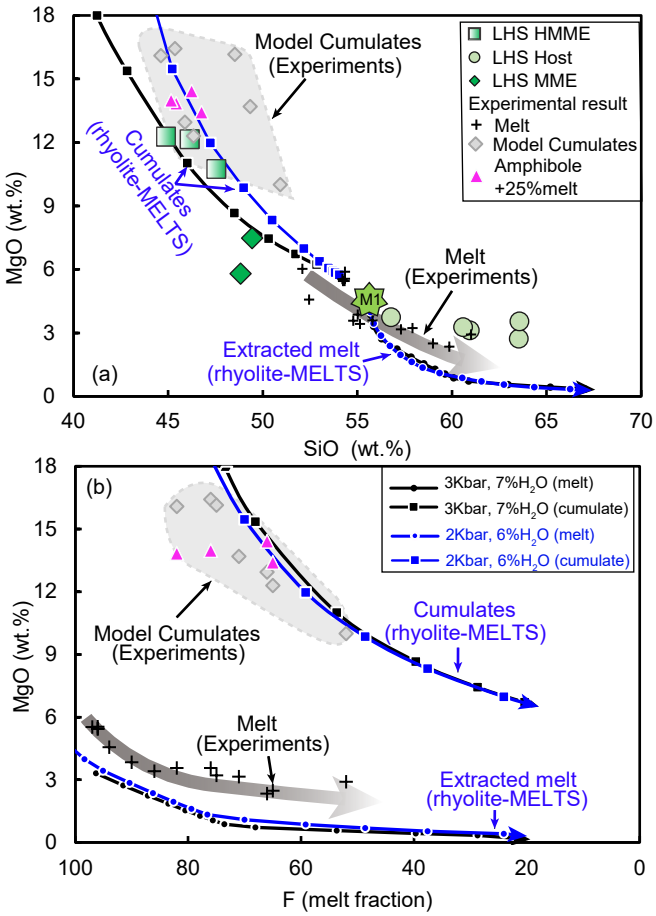

Journal of Petrology accepted manuscript - 2021-11-25

Figure 15

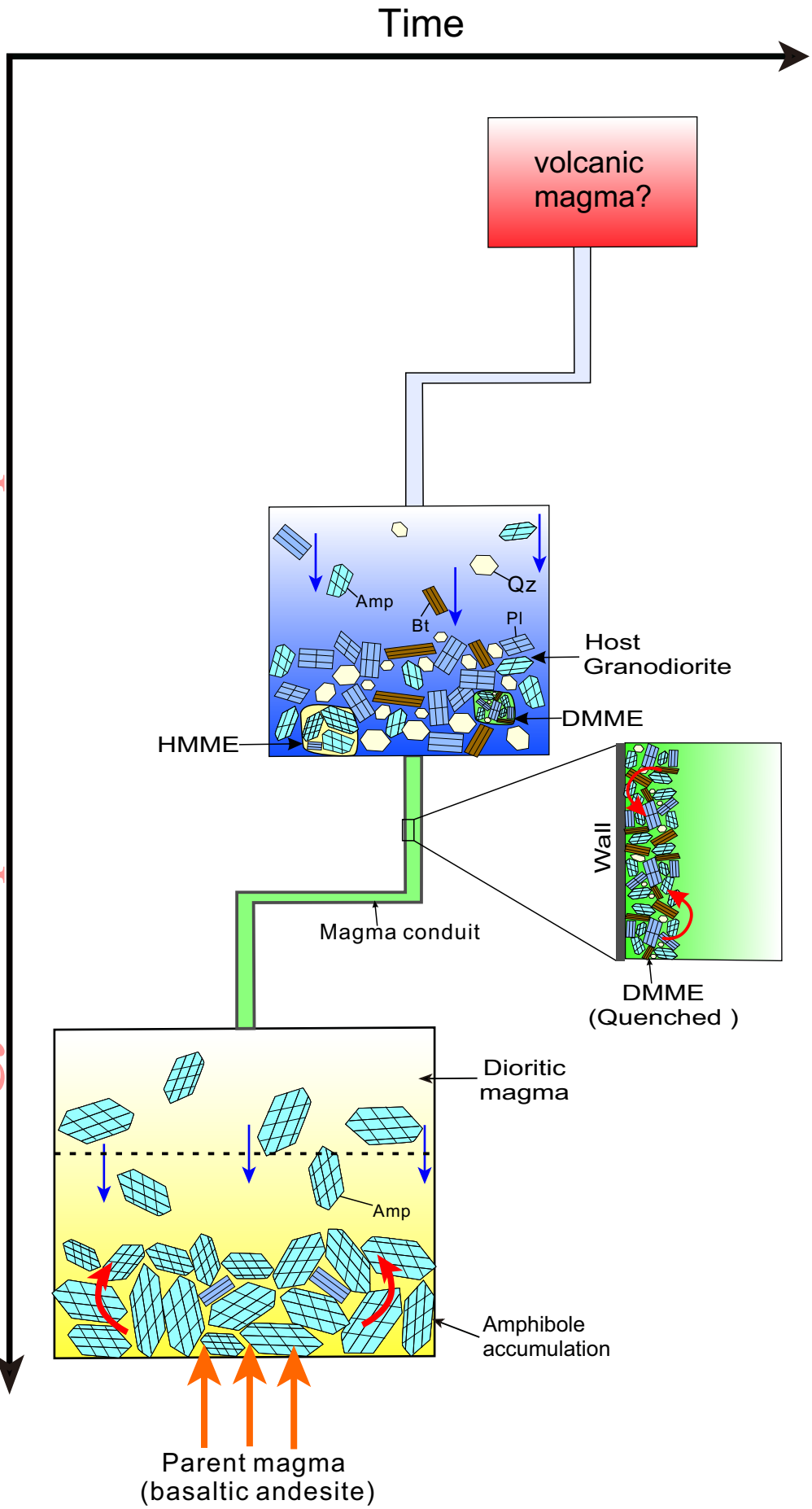

Journal of Petrology accepted manuscript - 2021-11-25

Journal of Petrology accepted manuscript - 2021-11-25

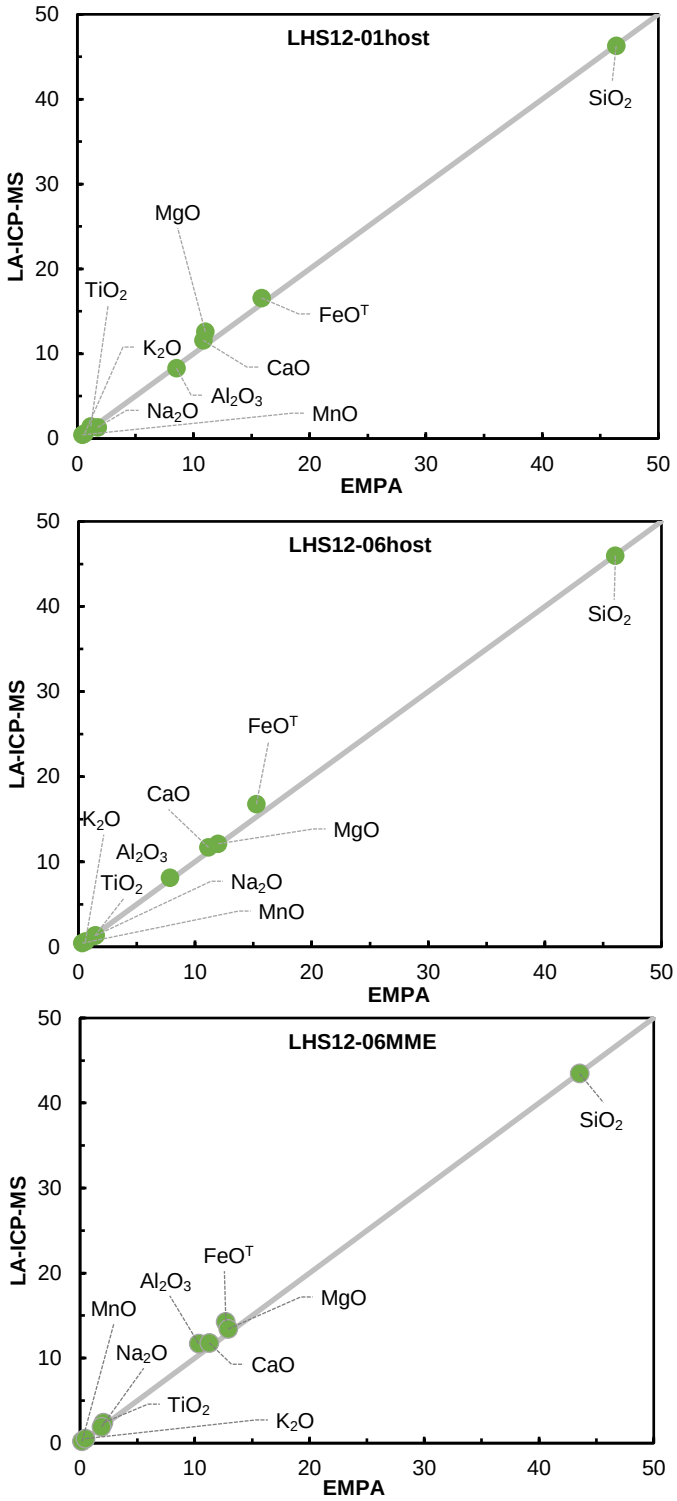

Figure S1. Comparison of major element contents obtained by LA-ICP-MS in this study with those previously obtained by EMPA (Chen et al., 2018).

Journal of Petrology accepted manuscript - 2021-11-25

Figure S2. Cathodoluminescene (CL) images of zircons from the host granitoids and their MMEs from NQOB. The red circles indicate the location of O isotope analyses.

Journal of Petrology accepted manuscript - 2021-11-25

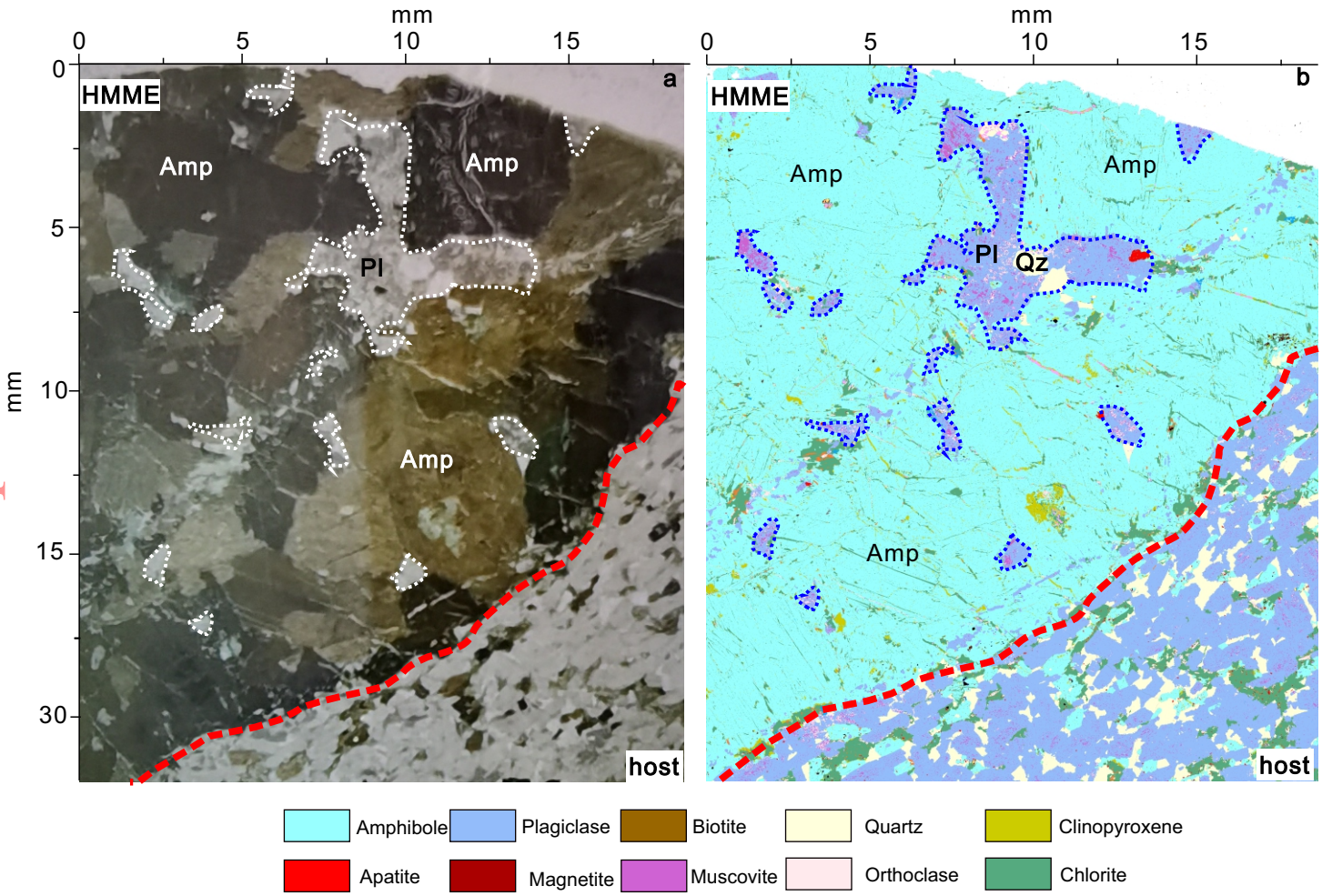

Figure S3. Thin section photos (a) and phase map imaged by TIMA (b) of LHS HMME and its granodiorite showing the HMME is dominated by idiomorphic amphibole with varying grain size and interstitial plagioclase (outlined by white and blue dashed lines). The red line shows the contact of HMME its host granodiorite.

Journal of Petrology accepted manuscript - 2021-11-25

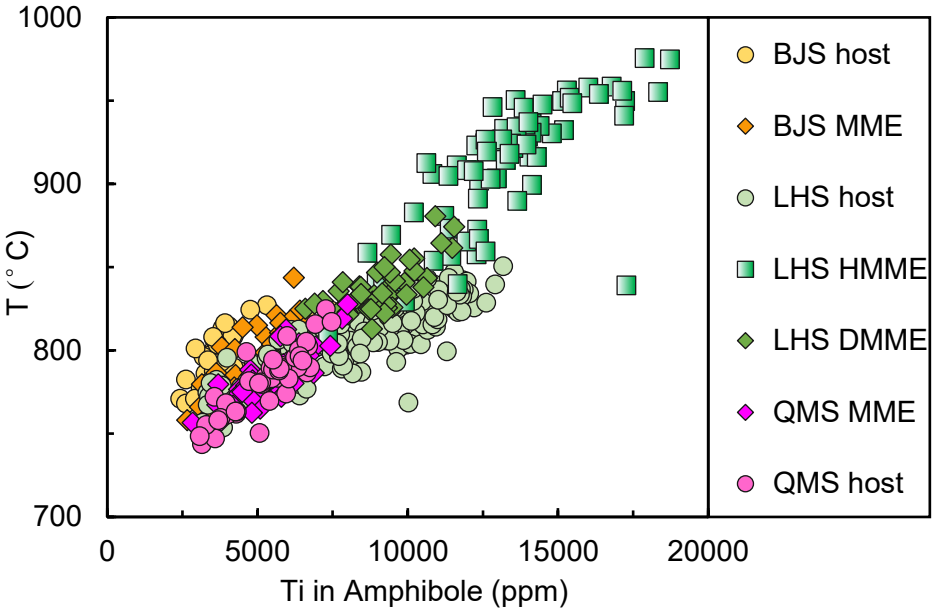

Figure S4: Variation of Ti as a function of temperature (T °C) in amphiboles. The temperature was calculated from Putirka (2016)